# Relationship between Stability and Function for Isolated Domains of Troponin C[†]

R. Scott Fredricksen[‡] and Charles A. Swenson*

*Department of Biochemistry, University of Iowa, Iowa City, Iowa 52242*

*Received May 29, 1996; Revised Manuscript Received August 27, 1996*[⊗]

ABSTRACT: Results of spectroscopic thermal and chemical denaturation studies and calcium binding studies are presented for a series of five recombinant chicken troponin C fragments. They were designed to assess the effects of domain isolation, N-helix, and D/E linker helix on stability and calcium affinity. Four of the fragments include the N-terminal regulatory domain and one the C-terminal domain. For the regulatory domain, deletion of the N-helix or the D/E linker decreases the stability of the apo form as measured by $\Delta G^{\circ}_{N\rightarrow U,25}$. Separation of the domains also decreases the stability. Differences in values of $\Delta G^{\circ}_{N\rightarrow U,25}$ derived from urea and guanidine hydrochloride studies allowed an estimation of the electrostatic component of the free energy of unfolding. Our measurements provide the first quantitative estimate of the stability for the apo-C-domain ($\Delta G^{\circ}_{N\rightarrow U,25} = -1.8$ kcal/mol) which was obtained using the interaction free energy formalism of Schellman. There is an inverse correlation between calcium affinity, binding cooperativity, and stability for all of these homologously structured fragments. The calcium affinity and cooperativity are highest for the unstructured C-domain and lowest for the N-domain which has the highest stability. In view of the direct effects on the folding stability of the apo-N-domain, the N-helix and the bilobed domain organization of TnC are necessarily involved in the fine-tuning of the affinity and cooperativity of calcium binding. Though not directly involved in calcium coordination, these structural features are important for signal transmission by troponin C in the troponin complex.

The calcium-dependent interactions between TnC[1] and TnI within holo-Tn are thought to represent the first steps of an allosteric switch (Grabarek *et al.*, 1992; Leavis & Gergely, 1984; Zot & Potter, 1987; Potter & Johnson, 1982) as they show the largest calcium dependence (Ingraham & Swenson, 1984; Wang & Cheung, 1985; Cheung *et al.*, 1987). A calcium-dependent competition between actin and TnC for the inhibitory peptide region of TnI is a key feature of current models of the mechanism of calcium signaling in the regulated thin filament (Talbot & Hodges, 1983; Dalgarno *et al.*, 1982; Cachia *et al.*, 1983; Grabarek *et al.*, 1986; Van Eyk & Hodges, 1988).

X-ray diffraction studies of turkey TnC reveal an extended, dumbbell-shaped structure with two globular domains connected by a nine turn α-helix (Herzberg & James, 1985, 1988). Recent NMR studies also show a two domain structure, but the connecting polypeptide chain (D/E linker) is unstructured (Slupsky & Sykes, 1995). The C-terminal domain of TnC binds a pair of calcium ions in an EF hand motif (Kretsinger & Nockolds, 1973) with high affinity (sites III and IV, $K_a \approx 2 \times 10^7$ M$^{-1}$) as well as magnesium ions with low affinity ($K_a \approx 4 \times 10^3$ M$^{-1}$; Zot & Potter, 1982; Potter & Gergely, 1975); it is thought to be involved in positioning TnC in Tn (Grabarek *et al.*, 1981; Zot & Potter, 1982; Negele *et al.*, 1992; Farah *et al.*, 1994). The N-terminal domain binds calcium ions with lower affinity (sites I and II, $K_a \approx 10^5$ M$^{-1}$) and is thought to be the site of the regulatory calcium-binding events. Recent NMR structural studies have demonstrated a bulk movement of helices B and C with little change in helical content on calcium binding (Gagné *et al.*, 1995). This exposes a hydrophobic pocket which is part of the antiparallel motif for the interaction of TnC with TnI and initiates signal transmission to the rest of the regulated thin filament (Farah *et al.*, 1994; Olah & Trewhella, 1994).

Studies using recombinant molecules have provided information on the functional importance of various structural components of TnC. The N-helix, while not directly involved in calcium binding, has been shown to be functionally important (Smith *et al.*, 1994; Li *et al.*, 1994; Chandra *et al.*, 1994; Gulati *et al.*, 1992; da Silva *et al.*, 1993). It is also a determinant of the functional difference between TnC and calmodulin (Gulati *et al.*, 1993, 1995). Results of studies of D/E linker mutants have shown that the spatial orientation of the two globular domains and the length of the linker helix are critically important for function (Babu *et al.*, 1993; Xu & Hitchcock-DeGregori, 1988; Dobrowolski *et al.*, 1991a,b; Sheng *et al.*, 1991; Ramakrishnan & Hitchcock-DeGregori, 1995; Gulati *et al.*, 1993).

In order to fully understand the relationship between TnC structure and its function as a molecular switch, knowledge of the energetic effects of calcium binding on stability and subunit−subunit interactions is required. Few studies have presented data which address the contribution of the N-helix, the D/E linker region, and ligand binding to the functional energetics of TnC. Hitchcock-DeGregori and co-workers

[†] Supported by a grant from the Muscular Dystrophy Association of America.

* To whom correspondence should be addressed. Phone: (319) 335-7917.

[‡] Present address: 5W-58 Brody Bldg., Department of Biochemistry, East Carolina University, Greenville, NC 27858.

[⊗] Abstract published in *Advance ACS Abstracts,* October 15, 1996.

[1] Abbreviations: ChTnC, chicken or turkey troponin C; ChTnC1−85, residues 1−85 of ChTnC; ChTnC12−85, residues 12−85 of ChTnC; ChTnC1−105, residues 1−105 of ChTnC; ChTnC12−105, residues 12−105 of ChTnC; DSC, differential scanning calorimetry; DTT, dithiothreitol; EGTA, ethylene glycol bis(2-aminoethyl ether)-*N*,*N*,*N*′,*N*′ tetraacetic acid; GndHCl, guanidine hydrochloride; NTA, nitrilotriacetic acid; TnC, troponin C, calcium binding subunit of troponin; TnI, troponin I, inhibitory subunit of troponin; TnT, troponin T, tropomyosin binding subunit of troponin.

S0006-2960(96)01270-6 CCC: $12.00 

have shown that deletion or insertion mutations within the D/E linker helix have minimal effects on the spectroscopically determined thermal transition midpoints for the globular domains within holo-ChTnC; deletion of part or all of the N-helix significantly affected the transition midpoints of the N-domain while having no effect on C-domain stability (Smith *et al*., 1994; Smith, 1995; Ramakrishnan & Hitchcock-DeGregori, 1995).

Results of calorimetric experiments (DSC) on tryptic fragments of rabbit TnC have been interpreted to suggest the presence of a destabilizing interaction between the two functional domains of holo-TnC (Tsalkova & Privalov, 1985). Such interactions would necessarily affect the energetics of calcium-dependent binding to TnI as well as other $(Ca)_x$−TnC interactions in the thin filament. Our own studies suggested a significant interaction between the N- and C-terminal domains of TnC when binding to TnI (Swenson & Fredricksen, 1992). This idea of interactions between TnC domains is supported by results of several other groups which showed that calcium binding to the C-terminal domain of holo-TnC affects spectroscopic probes in the N-domain (Wang *et al.*, 1990; Grabarek *et al.*, 1986; Tsuda *et al.*, 1988; Grabarek *et al.*, 1992). Detailed spectroscopic studies on tryptophan and tyrosine mutants of holo-TnC and isolated TnC domains showed that the N-domain retains the calcium-binding and structural features of TnC while the C-domain showed isolation-induced differences (Pearlstone *et al*., 1992; Li *et al*., 1994). In view of the obligatory relationship between protein structure and function, domain−domain interactions within TnC might play an important role in the molecular switching of skeletal muscle.

This paper presents the results of spectroscopic, thermal, and chemical denaturation studies and calcium binding studies on a series of five novel, recombinant ChTnC fragments which were designed to assess the effects of domain isolation, the N-helix, and the D/E linker region on protein stability and calcium affinity. Four of these protein fragments represent mutations of the N-domain of ChTnC. ChTnC1−85 represents the isolated N-domain. ChTnC12−85 is an N-helix deletion mutant of ChTnC1−85. ChTnC1−105 represents the N-domain plus D/E linker region to residue Phe105. ChTnC12−105 is an N-helix deletion mutant of ChTnC1−105. A fifth fragment, ChTnC95−162, represents an isolated C-domain. These results will be discussed in terms of the structural design of TnC as a molecular switch.

## EXPERIMENTAL PROCEDURES

### *Design and Construction of Recombinant ChTnC Protein Fragments*

Polymerase chain reaction (PCR) technology was used to generate cDNAs that coded for the five ChTnC protein fragments that were used in this study. The plasmid pUC120:ChTnC was the kind gift of Dr. Sarah Hitchcock-DeGregori (Xu & Hitchcock-DeGregori, 1988). The ChTnC cDNA was excised from the pUC120 plasmid by restriction digestion with *Nco*I and *Eco*RI and then subcloned into the *Nco*I/*Eco*RI site of the expression plasmid, pET3d (Studier *et al*., 1990). The pET3d:ChTnC plasmid was used as a template for all PCR work. In addition to defining the 5′ and 3′ ends of ChTnC fragment cDNAs for PCR-mediated amplification, the primer oligonucleotides were used to define two types of point mutations. For spectral analysis, ChTnC1−85 and ChTnC1−105 have Q7Y mutations and ChTnC12−85 and ChTnC12−105 have F13Y mutations. The ChTnC*x*−105 fragments also contain F102Y mutations. All of the tyrosine substitutions are considered to be conservative. Gln7 of chicken skeletal TnC is replaced by tyrosine in the bovine cardiac TnC sequence while Phe13 is replaced by tyrosine in rabbit, mouse, human, and pig skeletal TnCs. The skeletal TnCs from these species all contain phenylalanine at the equivalent of position 102. The ChTnC*x*−105 and ChTnC95−162 fragments contain corrected amino acid sequences at positions 99 and 100 (Ala99-Asn100) that replace a Glu99-Asp100 sequence which was coded for by the original cDNA (Xu & Hitchcock-DeGregori, 1988; Golosinska *et al*., 1991). The hot-start procedure for PCR was taken essentially from Sambrook *et al.* (1989).

After purification from the PCR reaction mixture, all ChTnC cDNAs were digested with *Nco*I and *Bam*HI, electrophoretically purified, and subcloned into *Nco*I/*Bam*HI sites of pET3d expression plasmids. All cDNA sequences were verified by the University of Iowa College of Medicine DNA Core using an Applied Biosystems (Division of Perkin-Elmer), Model 373A DNA sequencer.

All routine molecular biological methods (bacterial transformations, plasmid preparations, restriction enzyme digests, ligation reactions) were taken from Sambrook *et al*. (1989).

### *Protein Expression and Purification*

Expression plasmids for each of the ChTnC protein fragments were transformed into the *Escherichia coli* expression strain, BL21(DE3):pLysS (Studier et al., 1990). A recently transformed bacterial colony was used to inoculate 10 mL of LB medium containing ampicillin (0.2 mg/mL) and chloroamphenicol (0.03 mg/mL) which was then grown to saturation. This was used to inoculate 1 L of LB medium containing the same antibiotics.

The induction of protein expression and the purification of overexpressed ChTnC N-terminal protein fragments were carried out using the protocol of Xu and Hitchcock-DeGregori (1988). The procedure for purification of ChTnC95−162 was taken essentially from Li *et al.* (1994). Yields of lyophilized protein were ≈50 ± 10 mg/L of cell culture.

### *Tissue TnC Preparation*

Chicken and rabbit skeletal troponin were prepared from skeletal muscle ether powder following the procedures of Potter (1982) and Ingraham and Swenson (1984). Rabbit and chicken skeletal TnC, prepared from muscle tissue, were used interchangeably for all experiments.

### *Circular Dichroism Measurements*

Circular dichroism (CD) measurements for all of the TnC species were made on an Aviv 62DS circular dichroism spectrometer that was equipped with a thermoelectric temperature controller and an immersible thermocouple. Data were collected for four types of experiments: (1) far-UV wavelength spectra at 25 °C, (2) calcium titrations at 25 °C, (3) chemical denaturations at 25 °C, and (4) thermal denaturations. Raw data were converted to units of mean residue ellipticity, $[\theta]$ ($deg \cdot cm^2 \cdot dmol^{-1}$).

For spectra, stock solutions of protein samples were prepared in a 10 mM MOPS buffer, pH 7.25, containing 50 mM KCl, 1 mM DTT, and either (1) 2 mM $CaCl_2$, (2) 20 mM $MgCl_2$ and 0.2 mM EGTA, or (3) 0.1 mM EDTA. Data were averaged for three scans (260−200 nm) collected in 0.5 nm steps at 2 s/point, baseline corrected, and offset to zero signal between 250 and 260 nm. The spectra were smoothed using the Savitsky-Golay function (20%) of the Tablecurve graphics program.

Calcium titrations were performed using an EGTA/NTA calcium buffering system and were monitored by CD spectroscopy at 226 nm. A 2.4 mL aliquot, containing 5 $\mu$M protein in a pH 7.0 buffer solution (50 mM PIPES, pH 7.0, 0.1 M KCl, 1 mM EGTA, 1 mM NTA, 1 mM DTT, 0.01% $NaN_3$) at 25 °C, was titrated with a 10 mM $CaCl_2$ stock solution in an otherwise identical buffer. A BASIC computer program, using equations for a given total metal concentration that were solved simultaneously for the case of two ligands, was used to calculate free calcium concentrations (Perrin & Sayce, 1967). Absolute association constants of EGTA and NTA for protons and calcium were taken from Sillen and Martell (1964). The data, dilution-corrected signal versus free calcium concentration, were fit to two models of ligand binding (see Data Analysis).

Chemical denaturations, employing either urea or guanidine hydrochloride (GndHCl), were carried out on 15 $\mu$M protein samples in one of two ways. The first method entailed the titration of single protein samples with concentrated denaturant in a 2 mm Suprasil cuvette. After temperature equilibration at 25 °C, data were collected at 222 nm for 120 s and averaged. Control experiments showed that unfolding was complete in less than 1 min and that the circular dichroism signal was constant for at least 30 min. Dilution-corrected data were fit to two- or three-state models for unfolding.

As a second method for chemical denaturation experiments, discontinuous titrations were carried out using 24 samples per experiment. Two stock solutions at 15 $\mu$M protein were assembled: one in the absence of denaturant and the other in the presence of concentrated denaturant. Samples were prepared using different proportions of the stocks so that the widest range of denaturant concentration could be studied.

Thermal denaturations were performed on a 2.7 mL sample of 2.76 $\mu$M protein in a stirred 1 cm quartz cuvette equilibrated initially at 10 or 15 °C. The temperature was measured by an immersible plastic-coated thermocouple. Control experiments with scan rates ranging from 0.25 to 4 °C/min showed minimal effect on fit values of $\Delta H^{o}_{vh}$ and $T_m$. Thus the thermocouple response was adequate for the 1 °C/min heating rate used in these experiments. Macroprograms were used to (1) increase the temperature to a final set temperature of 88 or 95 °C and to (2) rapidly cool the sample. Spectral data at 222 nm were averaged for 15 s every 20 s and stored along with temperature data. The data were fit to a model for a two-state unfolding transition (see Data Analysis).

Reversibility of thermal denaturation was assessed by measuring the signal at native conditions after refolding at a rate of 1 °C/min to 0 °C. Percent renaturation was calculated from signal at 20 °C as follows:

$$\% \text{ renaturation} = \frac{\theta_d - \theta_f}{\theta_d - \theta_i} \times 100 \qquad (1)$$

where $\theta_d$ is the signal of the denatured protein extrapolated to 20 °C, $\theta_i$ is the initial signal at 20 °C, and $\theta_f$ is the signal of the renatured protein at 20 °C.

*UV Absorbance and Difference Spectrophotometry*

UV-vis spectra for all proteins were collected from 350 to 250 nm in 1 mm quartz cuvettes (Helma) on an Aviv 14DS UV−vis−IR dual-beam spectrophotometer at 25 °C. All spectra were corrected for the contribution of buffer components to signal.

Molar extinction coefficients for absorbance at 280 nm, $\epsilon^{native}_{280nm}$, were calculated for RbTnC and all of the recombinant ChTnC fragments using the procedure of Gill and von Hippel (1989).

Results of these measurements were used for calculation of native protein concentrations. The protein molecular weights, based on amino acid content, and $E^{1\%}_{280nm}$ values are as follows: RbTnC, MW = 17 313 g/mol, $E^{1\%}_{280nm}$ = 1.59; ChTnC1−85, MW = 9569 g/mol, $E^{1\%}_{280nm}$ = 1.44; ChTnC12−85, MW = 8342 g/mol, $E^{1\%}_{280nm}$=1.50; ChTnC1−105, MW = 11914 g/mol, $E^{1\%}_{280nm}$ = 2.42; ChTnC12−105, MW = 10688 g/mol, $E^{1\%}_{280nm}$ = 2.53; ChTnC95−162, MW = 8033 g/mol, $E^{1\%}_{280nm,apo}$ = 1.72, $E^{1\%}_{280nm,Mg}$ = 1.91, $E^{1\%}_{280nm,Ca}$ = 1.88.

*Differential Scanning Calorimetry*

Calorimetric measurements for the recombinant ChTnC1−85 protein were made over the temperature range 10−110 °C at a scanning rate of 1 °C/min on a DASM-1 scanning microcalorimeter which was extensively modified at the Biochemical Calorimetry Center at The Johns Hopkins University. The instrument was calibrated using van't Hoff and calorimetric enthalpy determinations from a series of lysozyme unfolding experiments at pH's of 2, 3, and 4 in 40 mM glycine buffer (Schwarz, 1989). Each experiment consisted of initial and repeat scans. Excess heat capacity data were recorded and analyzed by nonlinear least squares using the *cpplus6* program (E. Friere, Johns Hopkins University; see Data Analysis).

*Gel Electrophoresis*

All protein samples were analyzed on 12.4% or 15% SDS−PAGE using the Mini-Protean System (Bio-Rad Laboratories) which employs the Laemmli (1970) buffer system. The purity of the proteins was estimated to be greater than 95%. Plasmid DNA samples were analyzed by agarose gel electrophoresis on gels that were either 1% or 2% molecular biology grade agarose (International Biotechnologies, Inc.) or 1.5% Ultra-Pure low melting point agarose (Gibco BRL Life Technologies, Inc.). All gels were run using a flat-bed electrophoresis apparatus from Owl Scientific.

*Data Analysis*

*Protein Calcium Binding.* Macroscopic calcium dissociation constants were obtained by fitting the dilution-corrected signal versus $[Ca^{+2}]$ data to two models of ligand binding.

The first, Model A, is a Hill model which assumes a single set of identical ligand-binding sites per domain with cooperativity reflected in the magnitude of the Hill coefficient:

Model A:

$$y_i = \frac{y_m([Ca^{2+}]_i K_a)^H}{1 + ([Ca^{2+}]_i K_a)^H} \quad (2)$$

where $y_i$ is the fractional saturation after the $i$th addition, $y_m$ is the maximal signal change, $K_a$ is the macro-association constant, and $H$ is the Hill coefficient.

The second model, Model B, assumes two nonidentical ligand-binding sites per domain with cooperativity reflected in the magnitude of $K_2$, the macroscopic binding constant for binding two ligands to a given protein domain:

Model B:

$$y_i = \frac{y_m(K_1[Ca^{2+}] + 2K_2[Ca^{2+}]^2)}{2(1 + K_1[Ca^{2+}] + K_2[Ca^{2+}]^2)} \quad (3)$$

where $K_1$ is the macroscopic constant for binding of one ligand to a domain. A lower limit of the cooperative interaction free energy between binding sites, $\Delta G_c$, can be calculated by the following equation if it is assumed that the intrinsic site-binding constants are identical (Waltersson et al., 1993):

$$-\Delta G_c = RT \ln\left(\frac{4K_2}{K_1^2}\right) \quad (4)$$

where $R$ is the universal gas constant and $T$ is the temperature in K.

*Protein Stability. (A) Chemical Denaturation.* Baseline and transition region data for protein chemical denaturations were fit to either a two-state (Santoro & Bolen, 1992) or three-state (Morjana *et al.*, 1993) linear extrapolation model (LEM) based on the following equation:

$$\Delta G^o_{unfolding} = \Delta G^o_{H_2O} + m_g[\text{denaturant}] \quad (5)$$

where $\Delta G^o_{unfolding}$ is the standard free energy of unfolding for a given denaturant concentration, $\Delta G^o_{H_2O}$ is the standard free energy of unfolding in the absence of denaturant, and $m_g$ is a slope term which quantitates the change in $\Delta G^o_{unfolding}$ per unit concentration of denaturant. The models express signal as a function of denaturant concentration:

Two-State LEM:

Reaction: Native ↔ Denatured

$$y_i = \frac{y_N + m_N[X]_i + (y_D + m_D[X]_i)\exp[(-\Delta G^o_{H_2O} - m_g[X]_i)/RT]}{1 + \exp[(-\Delta G^o_{H_2O} - m_g[X]_i)/RT]} \quad (6)$$

where $y_i$ is the observed signal, $y_N$ and $y_D$ are the native and denatured baseline intercepts, $m_N$ and $m_D$ are the native and denatured baseline slopes, $[X]_i$ is the denaturant concentration after the $i$th addition, $\Delta G^o_{H_2O}$ is the extrapolated free energy of unfolding in the absence of denaturant, $m_g$ is the slope of a $G^o_{unfolding}$ vs [X] plot, $R$ is the gas constant, and $T$ is the temperature in K.

Three-State LEM:

Reaction: Native ↔ Intermediate ↔ Denatured

$$y_i = \{y_N + m_N[X]_i + y_i \exp[(-\Delta G^o_{NI} - m_{NI}[X]_i)/RT] + (y_D + m_D[X]_i)\exp[(-\Delta G^o_{NI} - m_{NI}[X]_i)/RT]\exp[(-\Delta G^o_{IU} - m_{IU}[X]_i)/RT]\}/\{1 + \exp[(-\Delta G^o_{NI} - m_{NI}[X]_i)/RT] + \exp[(-\Delta G^o_{NI} - m_{NI}[X]_i)/RT]\exp[(-\Delta G^o_{IU} - m_{IU}[X]_i)/RT]\} \quad (7)$$

where $y_i$ is the fitted value of ellipticity for the folding intermediate; $\Delta G^o_{NI}$ and $\Delta G^o_{IU}$ are the extrapolated free energies of unfolding in the absence of denaturant for the native to intermediate and intermediate to denatured transitions, respectively; $m_{NI}$ and $m_{ID}$ are the transition slope terms for the native to intermediate and intermediate to denatured transitions, respectively. The three-state LEM essentially models two sequential and independent two-state transitions. Some of the data sets did not contain sufficient baseline data to warrant the fitting of a baseline slope parameters (for either native or denatured baselines). For these cases, the appropriate baseline slope parameter was fixed at zero.

*(B) Thermal Denaturation.* Baseline and transition region data for thermal denaturations were fit to a two-state model (Santoro & Bolen, 1992) based on the following equation which returns the following as parameters of the fit: $\Delta H^o_{vh}$, van't Hoff enthalpy; $T_m$, temperature of the transition midpoint; the parameters $y_N$, $m_N$, $y_D$, $m_D$, $R$, and $T$ are as defined above.

$$y_i = \frac{y_N + m_N T + (y_D + m_D T)\exp\left[\frac{\Delta H^o_{vh}}{R}\left(\frac{1}{T_m} - \frac{1}{T}\right)\right]}{1 + \exp\left[\frac{\Delta H^o_{vh}}{R}\left(\frac{1}{T_m} - \frac{1}{T}\right)\right]} \quad (8)$$

*(C) Extrapolation of Free Energies of Unfolding.* Free energies and van't Hoff enthalpies of unfolding at a common temperature were calculated using the following equations, where $\Delta G°$, $T$, $T_m$, and $\Delta H^o_{vh,m}$ are defined as above.

$$\Delta G°(T) = \Delta H^o_{m,vh}(1 - T/T_m) - \Delta C_p(T_m - T + T\ln(T/T_m)) \quad (9)$$

$$\Delta H^o_{vh}(T) = \Delta H^o_{vh,m} + \Delta C_p(T - T_m) \quad (10)$$

An estimate of the denaturational change in heat capacity, $\Delta C_p$, that is needed for this extrapolation for ChTnC1−85 was determined from differential scanning calorimetric measurements. The value obtained, 360 ± 40 cal/(deg·mol), is in excellent agreement with the estimate of 400 cal/(deg·mol) obtained by Tsalkova and Privalov for the apo-N-terminal domain of RbTnC. The value of 360 cal/(mol·K) was used directly for ChTnC1−85.

Estimates of $\Delta C_p$ for all of the other recombinant apo-N-terminal domain ChTnC fragments were made from the

independently determined $\Delta C_p$ for ChTnC1−85, the $m_g$ values obtained from fits of chemical denaturation data to the Linear Extrapolation Model, and a derived relationship between them, $m_g/\Delta C_p = c$ (Alonso & Dill, 1991). The independently measured value of $\Delta C_p$ for apo-ChTnC1−85 permitted an estimation of the constant, *c*, using results from either GndHCl or urea chemical denaturation. The values of $\Delta C_p$ derived from urea denaturation data for ChTnC12−85, ChTnC1−105, and ChTnC12−105 were respectively 290, 310, and 290 cal/(deg·mol).

Estimates of $\Delta C_p$ for the magnesium- and calcium-bound forms of ChTnC95−162 were based on the direct calorimetric measurements of Tsalkova and Privalov (1980, 1985). We employed a value of 390 cal/(mol·K) for both the magnesium- and calcium-bound conformations of ChTnC95−162.

*Ligand Interaction Free Energy.* Ligands alter the stability of proteins by binding to the native and/or denatured states. The change in stability resulting from ligand binding is termed the interaction free energy, $\Delta G_b$, as derived by Schellman (1975):

$$\Delta G_b = -RT \ln \Sigma \quad (11)$$

where *R* is the universal gas constant, *T* is the temperature in K, and $\sum$ is the binding polynomial for the ligand to that state. For the two-state case, the net interaction free energy for the process is the difference in interaction free energies for the native and denatured states, $\Delta G_{b(D)} - \Delta G_{b(N)}$. Assuming that the ligand binds to a pair of independent and identical binding sites only in the native state, the net interaction free energy is stabilizing and is given by $-RT \ln(1/\sum_N) = -RT \ln(1/(1 + k_{Ca,n}[L])^2)$.

*Calorimetry.* Differential scanning microcalorimetry data were fit to a two-state model of unfolding using a program, *cpplus6*, developed by E. Friere (Johns Hopkins University). The general form of this model is:

$$\langle \Delta C_p \rangle = \left(\frac{K}{(1+K)^2}\right)\left(\frac{(\Delta H^o)^2}{R(T)^2}\right) + \frac{K}{(1+K)}\Delta C_p \quad (12)$$

where $\langle \Delta C_p \rangle$ is the measured excess heat capacity, *K* is the equilibrium constant for the unfolding reaction, $\Delta H^o$ is the standard calorimetric enthalpy of unfolding, *R* is the universal gas constant, *T* is the temperature in K, and $\Delta C_p$ is the denaturational change in heat capacity. The van't Hoff enthalpy, $\Delta H^o_{vh}$, is calculated as:

$$\Delta H^o_{vh} = 4R(T_{1/2})^2 \frac{C_{p,1/2}}{\Delta H^o} \quad (13)$$

where $T_{1/2}$ is the temperature, in K, at the peak of the excess heat capacity curve, and $C_{p,1/2}$ is the value of the excess heat capacity at $T_{1/2}$.

## RESULTS

### *Circular Dichroism*

CD spectral scans for selected ChTnC fragments are presented in Figure 1. Spectra for each of the N-domain ChTnC fragments showed negative peaks near 208 and 222 nm, characteristic of significant α-helical content in either the presence or absence of $Ca^{2+}$ or $Mg^{2+}$. Signal changes

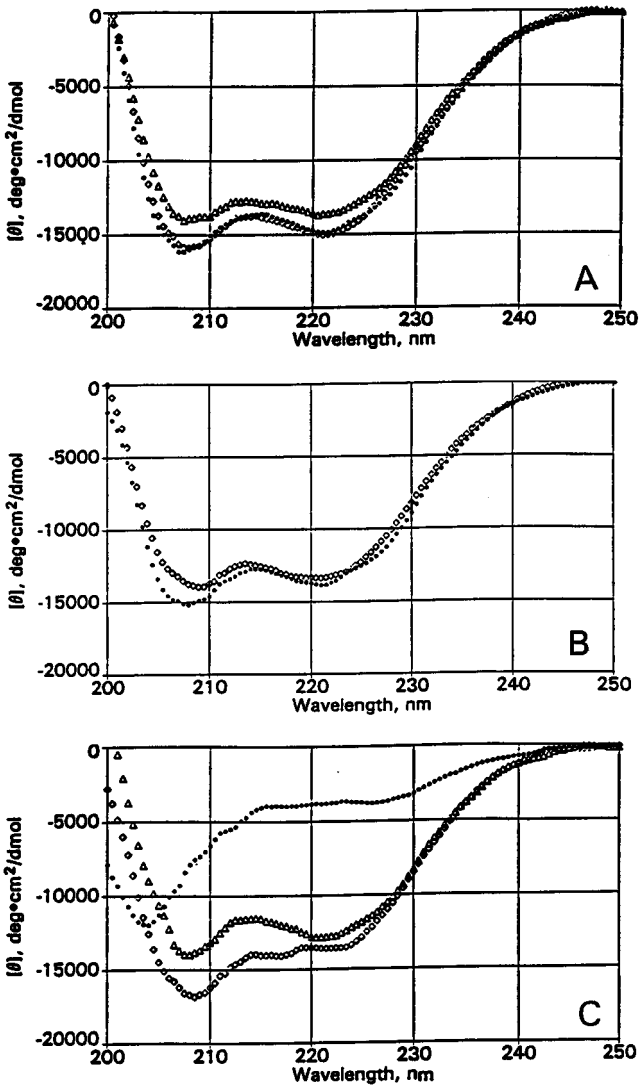


FIGURE 1: Far-UV CD spectra of recombinant ChTnC fragments. Solution conditions: 10 mM MOPS, pH 7.25, 50 mM KCl, 1 mM DTT, and either (1) calcium = 2 mM $CaCl_2$, (2) magnesium = 20 mM $MgCl_2$, 1 mM EGTA, or (3) EDTA = 1 mM EDTA. Protein concentrations were 20 $\mu$M. Symbol legends: ● ≡ EDTA; △ ≡ magnesium; ◇ ≡ calcium. Panel A: ChTnC1−85. Panel B: ChTnC12−85. Panel C: ChTnC95−162.

due to calcium binding varied significantly for the apo-N-domain fragments. ChTnC1−85 showed a small decrease in $[\theta]_{222}$ when measured in the presence of 2 mM $CaCl_2$ while ChTnC12−85, the N-helix-deletion mutant, showed a slight calcium-induced increase in $[\theta]_{222}$ For ChTnC1−105, however, a significant decrease in $[\theta]_{222}$ of approximately 3490 deg·cm²·dmol$^{-1}$ was observed when calcium was bound; the N-helix mutant ChTnC12−105 showed a decrease of ≈890 deg·cm²·dmol$^{-1}$. Interestingly, the presence of 20 mM $MgCl_2$ and 1 mM EGTA (i.e., calcium-free conditions) induced a significant signal increase for ChTnC1−85 ($\Delta[\theta]_{222} \approx 1100$ deg·cm²·dmol$^{-1}$). This protein fragment is expected to interact only weakly with magnesium ion. Spectra collected for apo-ChTnC1−85 in the presence of 100 mM KCl (equivalent in ionic strength to 50 mM KCl and 20 mM $MgCl_2$) showed slightly more *negative* signal at 222 nm and 208 nm ($\Delta[\theta]_{222} \approx -500$ deg·cm²·dmol-$^{-1}$). This suggests that the $MgCl_2$-induced increase in signal is a specific effect of magnesium.

The ligand-dependent changes in $[\theta]_{222}$ for ChTnC95−162 are consistent with its identity as the calcium/magnesium

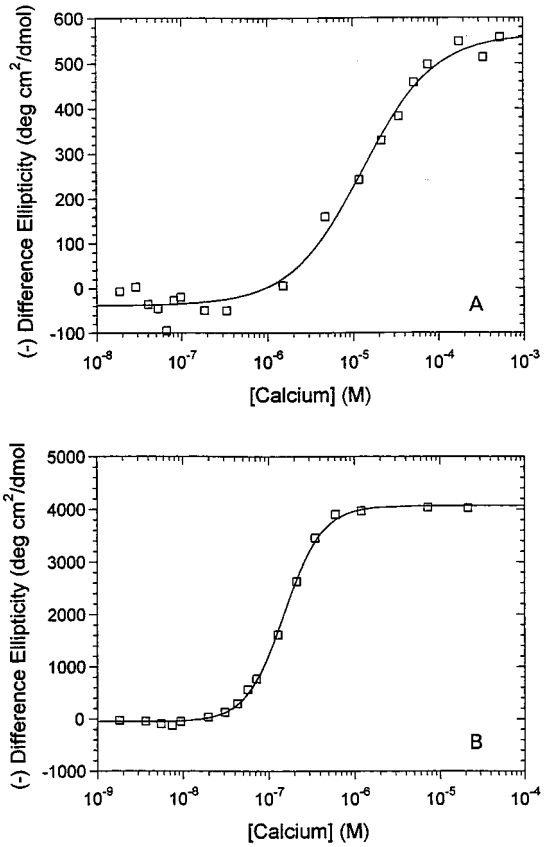


FIGURE 2: Calcium titrations of recombinant ChTnC fragments. Each data panel presents the change $[\theta]_{226nm}$ versus log[free calcium]. Protein samples at 2 $\mu$M were prepared in a calcium buffer consisting of 50 mM Pipes, pH 7.0, and 0.1 M KCl, 1 mM EGTA, 1 mM NTA, and 1 mM DTT. The titrant was 10 mM $CaCl_2$ in the same buffer. The data were fit to eq 2 (see Table 1). Panel A: ChTnC1−85. Panel B: ChTnC95−162.

binding domain of ChTnC. In the presence of EDTA, the CD spectra of ChTnC95−162 showed a broad plateau (≈−3800 deg·cm$^2$·dmol$^{-1}$) between 225 and 215 nm and a peak near 204 nm. In the presence of either 2 mM $CaCl_2$ or 20 mM $MgCl_2$ and 1 mM EGTA the shape of the ChTnC95−162 spectrum changed dramatically; negative peaks near 222 and 208 nm suggest the presence of a significant amount of ligand-induced α-helical structure. The magnitude of $[\theta]_{222}$ for ChTnC95−162 in the presence of 2 mM $CaCl_2$ is ≈850 deg·cm$^2$·dmol$^{-1}$ larger than that measured in the presence of 20 mM $MgCl_2$ and 1 mM EGTA.

### *Calcium Binding*

*ChTnC N-Domain Fragments.* Results of calcium binding experiments are presented in Figure 2 and Table 1. The fit of the data to Model A suggested that N-domain isolation had no effect on the calcium affinity of ChTnC1−85 ($K_a \approx (2.4 \pm 0.1) \times 10^5$ M$^{-1}$) or on the apparent cooperativity of binding ($H = 1.4 \pm 0.1$) (reference values for the N-terminal domain of ChTnC are $K_a = 2.3 \times 10^5$ M$^{-1}$, $H = 1.4$ from Smith *et al.*, 1994). Deletion of the N-helix from ChTnC1−85 resulted in an approximate 50% increase in calcium affinity ($K_a = (3.5 \pm 0.8) \times 10^5$ M$^{-1}$, Model A) and an increased index of cooperativity ($H = 1.6 \pm 0.2$) for ChTnC12−85.

Addition of residues 86−105 to ChTnC1−85 resulted in a $K_a \approx 8.6 \times 10^4$ M$^{-1}$; this value of $K_a$ is about 1/3 that for ChTnC1−85. The Hill coefficient for ChTnC1−105 was significantly lower than that for ChTnC1−85; the value of $H = 1$ suggests a complete absence of ligand binding cooperativity. Deletion of the N-helix from ChTnC1−105 resulted in an approximate 2.6-fold increase in $K_a$ and 1.3-fold increase in $H$ for ChTnC12−105 compared to ChTnC1−105 ($K_{a,ChTnC12-105} \approx 1.9 \times 10^5$ M$^{-1}$, $H_{ChTnC12-105} \approx 1.3$).

Overall, the results of fits of calcium binding data to a Hill equation (Model A) indicate that (1) neither the N-helix nor the D/E linker region is required for calcium binding, (2) N-helix deletion increases $K_a$ and $H$, and (3) the D/E linker decreases $K_a$ and $H$.

Fitting the data to Model B provided a different view of the effects of the N-helix and D/E linker region on calcium binding. Values of $K_1$, the macroscopic constant for binding of the first calcium ligand, are the same within experimental error for all the N-terminal fragments. This is in contrast to the differences suggested by values of $K_a$ (Model A). Differences in calcium binding for the N-domain fragments were evidenced by differences in the magnitudes of $K_2$ and $\Delta G_c$. Deletion of the N-helix from ChTnC1−85 resulted in a decrease in $\Delta G_c$ of ≈1.2 kcal/mol; N-helix deletion from ChTnC1−105 resulted in a similar decrease of ≈1.1 kcal/mol. Addition of residues 86−105, on the other hand, resulted in a $\Delta G_c$ of ≈+0.9 kcal/mol for the ChTnC1−$x$ fragments and $\Delta G_c$ of ≈+1.0 kcal/mol for the CnTnC12−$x$ fragments. The values of $K_1$ and $K_2$ for ChTnC1−85 are in good agreement with those recently determined for similar fragments using multidimensional NMR techniques (Li *et al.*, 1995).

*ChTnC95−162.* The calcium affinity constant of ChTnC95−162, from fits to Model A, was equal to $6.3 \times 10^6$ M$^{-1}$. This value is in excellent agreement with the value of $6.5 \times 10^6$ obtained by Li *et al.* (1994). Calcium binding to ChTnC95−162 is a highly cooperative phenomena with $H \approx 2$ (Model A) and a cooperative free energy of binding $\Delta G_c \approx -2.5$ kcal/mol (Model B). Smith *et al.* (1994) reported a slightly larger value for $K_a$ of $2.3 \times 10^7$ M$^{-1}$ for the C-domain of holo-ChTnC.

### *Thermal Denaturation*

*Reversibility and Validation of Two-State Model for TnC Fragments.* Figure 3 illustrates the reversibility of unfolding for two of the apo-recombinant N-terminal domain fragments, ChTnC1−85 and ChTnC12−85, and for $Ca_2$-ChTnC95−162. Reversibility of thermal unfolding was assessed by measuring the percent recovery of initial signal after refolding at the same scan rate as for unfolding. The percent of unfolded protein that refolded was estimated using eq 1. The range of percent renaturation for the apo-N-domain fragments was 88−96%. The thermal unfolding of $Ca_2$-ChTnC95−162 was ≈93% reversible.

Temperature-dependent CD spectra for all of the ChTnC fragments demonstrated an isodichroic point at 204 nm, consistent with a two-state transition. Figure 4 presents the spectra for a representative apo-N-domain fragment, ChTnC1−85, and for $Ca_2$-ChTnC95−162. Additional support for a two-state mechanism of unfolding for ligand-free ChTnC N-domain fragments is based on the analysis of preliminary DSC results for apo-ChTnC1−85. The ratio of $\Delta H^o_{vh}$ to $\Delta H^o_{cal}$ was very close to 1 ($\Delta H^o_{cal,\ 25°C} = 36.2 \pm 2.5$ kcal/mol, $\Delta H^o_{vh,\ 25°C} = 36.4 \pm 2.3$ kcal/mol).

Table 1: Calcium-Binding Parameters for TnC Fragments[a]

| | | Model A[b] | | Model B[c] | | |
|---|---|---|---|---|---|---|
| protein | $N$ | $K_{Ca} \times 10^{-5}$, $M^{-1}$ | $H_a$ | $K_1 \times 10^{-5}$, $M^{-1}$ | $K_2 \times 10^{-10}$, $M^{-2}$ | $\Delta G_c$[d] |
| ChTnC1−85 | 4 | 2.4 ± 0.1 | 1.4 ± 0.1 | 2.8 ± 0.4 | 5.3 ± 0.7 | −0.6 ± 0.2 |
| ChTnC12−85 | 3 | 3.5 ± 0.8 | 1.6 ± 0.2 | 1.8 ± 0.6 | 16.0 ± 7.0 | −1.8 ± 0.7 |
| ChTnC1−105 | 2 | 0.86 ± 0.14 | 1.0 ± 0.1 | 2.2 ± 0.9 | 0.77 ± 0.36 | +0.3 ± 0.8 |
| ChTnC12−105 | 1 | 1.9 | 1.3 | 1.9 | 3.6 | −0.8 |
| ChTnC95−162 | 3 | 63.0 ± 4.0 | 2.1 ± 0.1 | 15.0 ± 7.0 | 4000.0 ± 500.0 | −2.5 ± 0.6 |

[a] Ranges for parameters are ± student standard deviations. Buffer conditions can be found in the legend of Figure 2. [b] Model A is eq 2. [c] Model B is eq 3. [d] Units of $\Delta G_c$ = kcal/mol; $\Delta G_c$ represents an estimate of the lower limit of the cooperative free energy of binding two ligands and is calculated as $-RT \ln(4K_2/(K_1)^2)$.

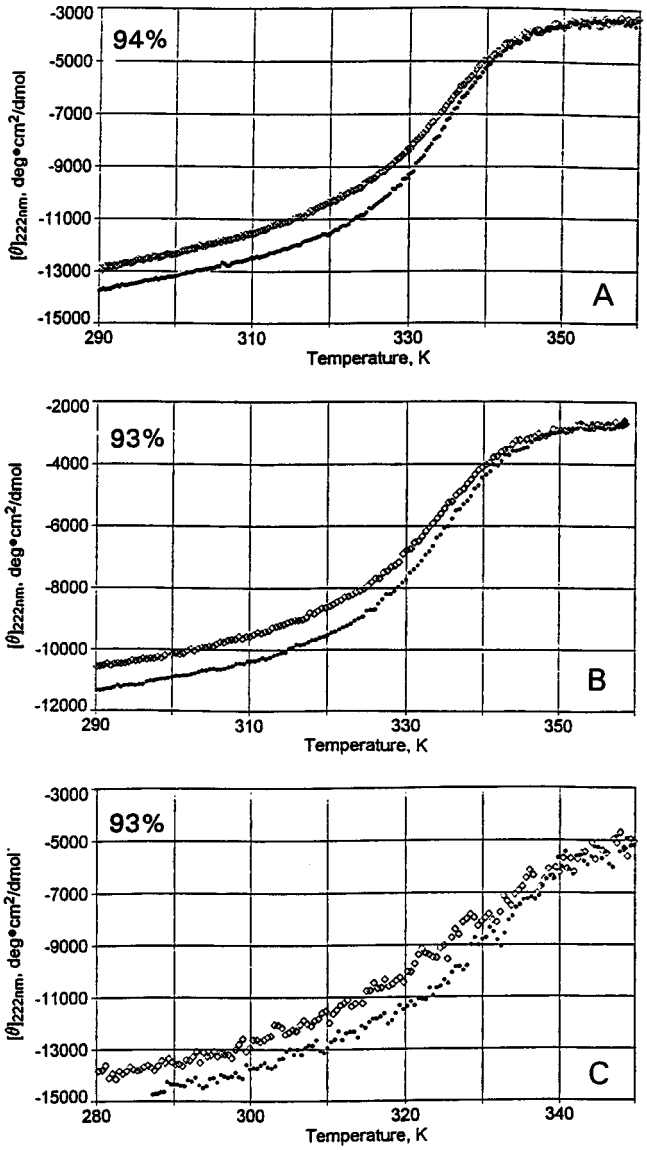


FIGURE 3: Reversibility of thermal denaturation. Recombinant N-domain ChTnC fragments, in the absence of ligands, and calcium-bound ChTnC95−162 were thermally unfolded at a heating rate of 1 °C/min (●) starting at 10 °C. After reaching the maximum temperature, the samples were cooled at 1 °C/min to a final temperature of 1 °C (◊). The protein concentrations were 2.76 $\mu$M. The percent renaturation, calculated using eq 1, is indicated in each panel. The buffer was 10 mM MOPS, pH 7.25, 50 mM KCl, 1 mM DTT, and either (1) 1 mM EDTA for panels A and B or (2) 2 mM $CaCl_2$ for panel C. Panel A: apo-ChTnC1−85. Panel B: apo-ChTnC12−85. Panel C: $Ca_2$-ChTnC95−162.

*Thermodynamic Parameters of CD-Monitored Thermal Denaturation.* Typical CD-monitored thermal scans for the unfolding of ChTnC and ChTnC fragments, along with fits to a two-state model of unfolding, are presented in Table 2 and Figure 5. Isolation of the N-domain of ChTnC as ChTnC1−85 or ChTnC1−105 had little effect on the van't Hoff enthalpy of unfolding extrapolated to 25 °C. Values of $\Delta H^o_{vh,\ 25°C}$ for ChTnC, ChTnC1−85, and ChTnC1−105 fall within a range of ≈4 kcal/mol. The transition midpoints and, hence, values of $\Delta G^o_{25}$ were very sensitive to deletion of residues 106−162 or 86−162. A similar observation was made for the ChTnC12−$x$ fragments; values of $\Delta H^o_{vh,\ 25°C}$ for this pair of proteins are similar and are ≈10−11 kcal/mol less than corresponding values for the ChTnC1−$x$

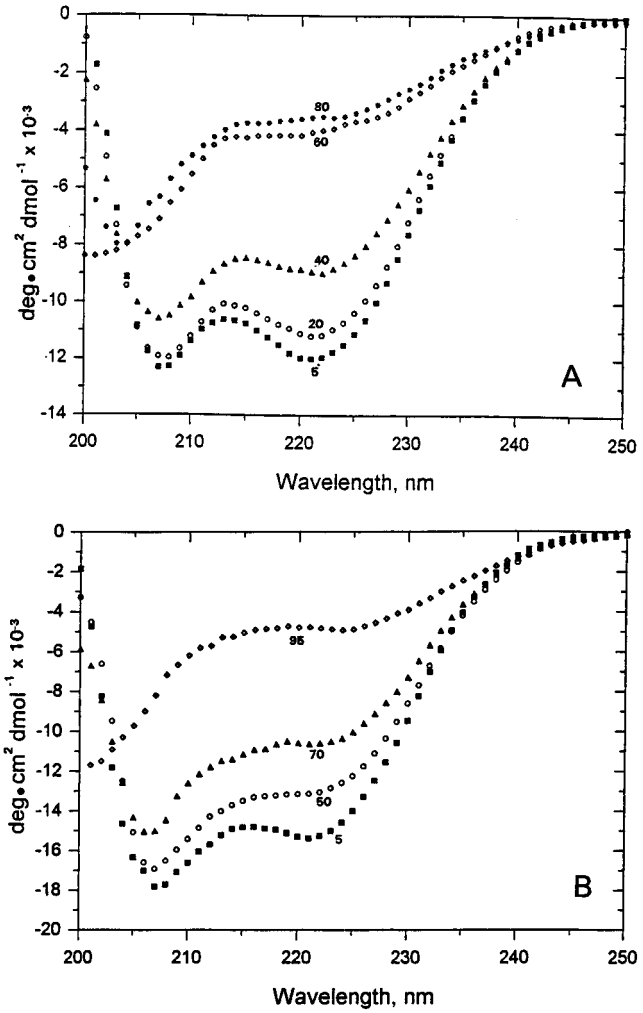


FIGURE 4: Temperature dependence of typical circular dichroism spectra for ChTnC fragments. Circular dichroism spectra were collected for 20 $\mu$M protein samples in 1 mm quartz cells at the temperatures indicated. Sample buffer: 10 mM MOPS, pH 7.25, 50 mM KCl, and either 1 mM EDTA (panel A) or 50 $\mu$M total $CaCl_2$ (panel B). Panel A: apo-ChTnC1−85 at 5, 20, 40, 60, and 80 °C. Panel B: $Ca_2$-ChTnC95−162 at 5, 50, 70, and 95 °C.

Table 2: Thermal Stability Parameters for TnC and ChTnC Fragments[a]

| parameters | ChTnC1−85 | ChTnC12−85 | ChTnC1−105 | ChTnC12−105 | ChTnC | dRbTnC[e] | TR1[e] |
|---|---|---|---|---|---|---|---|
| $\Delta G^{o}_{25}$ [b] | 2.6 ± 0.1 | 1.6 ± 0.1 | 5.1 ± 0.1 | 2.9 ± 0.1 | 4.8 ± 0.1 | 4.8 | 4.2 |
| $\Delta H^{o}_{vh,25}$ | 37.5 ± 1.2 | 27.1 ± 1.2 | 36.8 ± 0.2 | 25.3 ± 1.4 | 41.0 ± 2.2 | 43.4 | 43.4 |
| $T_m$, K | 45.2 ± 0.4 | 41.8 ± 0.2 | 65.4 ± 0.1 | 56.7 ± 0.1 | 59.1 ± 0.7 | 57 | 54 |
| n[d] | 6 | 4 | 3 | 3 | 3 | NG[f] | NG[f] |

| parameters | ChTnC95−162 | parameters | ChTnC95−162 |
|---|---|---|---|
| $\Delta G^{o}_{25}$ [b] | 3.6 | $\Delta G^{o}_{25}$ | 2.4 ± 0.2 |
| $\Delta H^{o}_{vh,25}$ [c] | 17.1 | $\Delta H^{o}_{vh,25}$ | 15.7 ± 2.4 |
| $T_m$, °C | 72.4 | $T_m$, °C | 60.5 ± 1.3 |
| [calcium], $\mu$M | 15 | [magnesium], mM | 20 |
| n[d] | 1 | n | 4 |

[a] Ranges for parameters are ± student standard deviation. Solution conditions for ChTnC and ChTnC N-domain fragments: 10 mM MOPS, pH 7.25, 50 mM KCl, 1 mM EDTA, 1 mM DTT; protein concentrations were 2.76 $\mu$M. Solution conditions for ChTnC95−162: 10 mM MOPS, pH 7.25, 50 mM KCl, 1 mM DTT, and either 15 $\mu$M $CaCl_2$ or 20 mM $MgCl_2$, 1 mM EGTA. Protein concentrations were 2.76 $\mu$M. Solution conditions for RbTnC and TR1: 10 mM cacodylate, pH 7.25, 2 mM EDTA. Protein concentrations were between 90 and 300 $\mu$M. [b] Units of $\Delta G^{o}_{25}$ = kcal/mol; values calculated using eq 9. The values of $\Delta C_p$ which were used in calculating $\Delta G^{o}_{25}$ are 360, 290, 310, 290, and 390 cal/(deg·mol), respectively, for ChTnC1−85, ChTnC12−85, ChTnC1−105, ChTnC12−105, and ChTnC95−162. The value of $\Delta C_p$ for RbTnC was taken from Tsalkova and Privalov (1980); the value of $\Delta C_p$ for TR1 was set equal to that for ChTnC12−85 since the two proteins are nearly identical. [c] Units of $\Delta H^{o}_{vh,25}$ are kcal/mol; values calculated from eq 10. [d] Number of trials. [e] Parameters calculated using data from Tables 1 and 3 of Tsalkova and Privalov (1985); protein concentrations in these experiments were ≈60−100 times higher than for ChTnC or ChTnC fragments. [f] Not given.

fragments. Values of $T_m$ and $\Delta G^{o}_{25}$ are also sensitive to the presence of residues 86−105. The trend of free energies of unfolding at 25 °C ($\Delta G^{o}_{25}$) for apo-N-domain proteins at 2.76 $\mu$M is ChTnC1−105 > ChTnC > ChTnC12−105 > ChTnC1−85 > ChTnC12−85. The values of $T_m$, $\Delta H^{o}_{vh,25}$, and $\Delta G^{o}_{25}$ for the single transition of ChTnC (Table 2 and Figure 5) are essentially identical to values reported by Tsalkova and Privalov (1980, 1985). The last two columns of Table 2 present results of calculations of $\Delta G^{o}_{25}$ and $\Delta H^{o}_{vh,25}$ for RbTnC and TR1, an N-terminal fragment of TnC, based on data from Tables 1 and 3 of Tsalkova and Privalov (1985).

Interestingly, the effect of an N-helix deletion on $\Delta H^{o}_{vh,25}$ and $\Delta G^{o}_{25}$ depends on the presence of the D/E linker region; $\Delta\Delta H^{o}_{vh,25} \approx -10.4$ kcal/mol and $\Delta\Delta G^{o}_{25} \approx -1$ kcal/mol for N-helix deletion from ChTnC1−85; $\Delta\Delta H^{o}_{vh,25} \approx -11.5$ kcal/mol and $\Delta\Delta G^{o}_{25} \approx -2.2$ kcal/mol for N-helix deletion from ChTnC1−105. Similarly, for D/E linker deletion, $\Delta\Delta H^{o}_{vh,25} \approx 0.7$ kcal/mol and $\Delta\Delta G^{o}_{25} \approx -2.5$ kcal/mol for the ChTnC1−*x* fragments while $\Delta\Delta H^{o}_{vh,25} \approx 1.8$ kcal/mol and $\Delta\Delta G^{o}_{25} \approx -1.3$ kcal/mol for the ChTnC12−*x* fragments. These results suggest the presence of an interaction between these two stretches of primary structure.

Thermal unfolding of the apo-ChTnC95−162 fragment showed no detectable transition. Results of two-state analysis of thermal unfolding curves for the calcium- and magnesium-bound forms of this protein are presented Table 2. The near identical values of $\Delta H^{o}_{vh,25}$ for $Mg_2$-ChTnC95−162 and $Ca_2$-ChTnC95−162 are significantly less than the values for any of the apo-N-domain fragments.

*Free Energies of Unfolding and Ligand Affinities.* The difference in free energy of unfolding measured in the presence and absence of ligand is defined by the following equation, which is derived from eq 11 for a two-state model for unfolding.

$$\Delta G^{o}_{25,Ca} - \Delta G^{o}_{25,apo} = -RT \ln(1/\Sigma_N) = -RT \ln(1/(1 + k_{Ca,n}[Ca])^2) \quad (14)$$

Using the measured free energies of unfolding at 25 °C in the presence and absence of calcium ion, presented in Tables 3 and 2, respectively, the calcium binding constants presented in column five of Table 3 were calculated. The binding polynomial used assumes two identical, independent sites and seems appropriate as it modeled direct calcium binding to all the fragments well. The ligand binding constants are in excellent agreement with direct calcium binding experiments.

From data similar to that given in Table 3, but for magnesium, the value of $K_{Mg}$ for ChTnC1−85 was estimated to be ≈440 $M^{-1}$. This confirms the limited spectroscopic evidence (Figure 1) that suggests that the N-terminal domain of TnC is able to weakly bind magnesium ions (Tsuda *et al.*, 1990).

The free energy of unfolding for apo-ChTnC95−162 at 25 °C is not directly measurable as this fragment is largely unstructured. This free energy was calculated using eq 14, the directly measured values of $K_1$ and $K_2$ in the binding polynomial $1 + K_1[Ca^{2+}] + K_2[Ca^{2+}]^2$, and the unfolding free energy of ≈3.6 kcal/mol which was determined in the presence of ≈15 $\mu$M free calcium (Table 2). The calculated $\Delta G^{o}_{25,apo}$ for ChTnC95−162 of −1.8 kcal/mol corresponds to an equilibrium constant of ≈20; thus this fragment is ≈95% unfolded at 25 °C.

*Chemical Denaturation*

Chemical denaturation studies, using urea and GndHCl as denaturants, were performed for all of the recombinant ChTnC fragments and RbTnC. All chemical denaturations were judged to be reversible based on the high recovery of the initial CD signal (>98% for the N-domain fragments; 90−95% for ligand-bound ChTnC95−162) after dilution to nondenaturing concentrations of denaturant. The data were fit to either a two-state LEM (all ChTnC fragments) or a three-state LEM (RbTnC) which models unfolding as a sequence of two independent two-state unfolding reactions (eq 6 or 7, respectively). Figure 6 shows fitted chemical denaturation curves for the ChTnC*x*−85 fragments and for RbTnC. Table 4 summarizes the results of LEM analysis for these proteins.

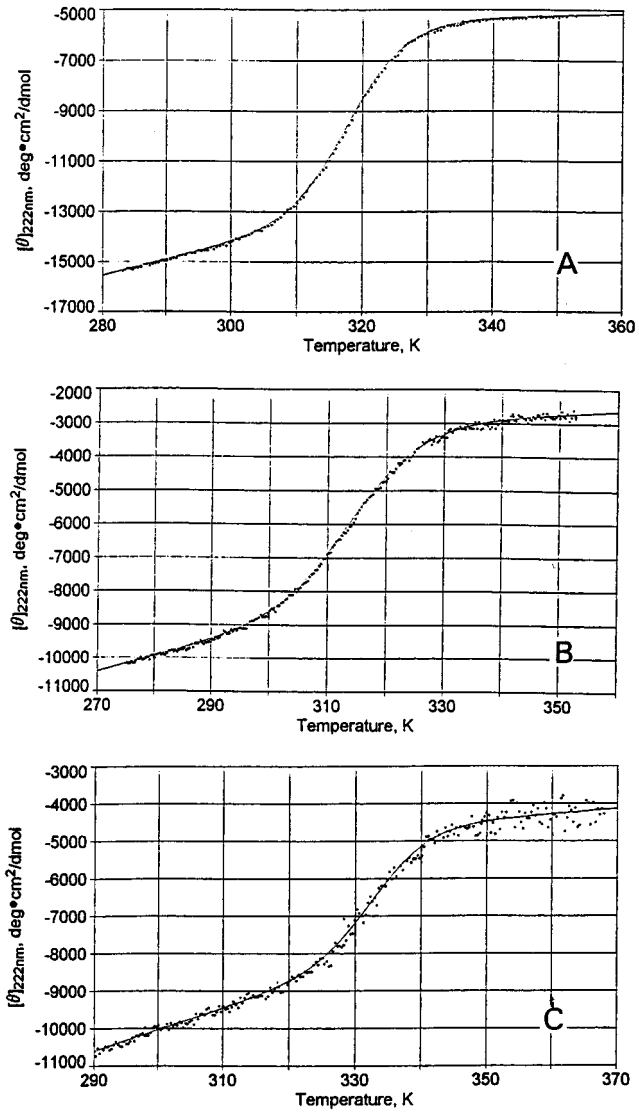


FIGURE 5: Thermal denaturations of ChTnC1−85, ChTnC12−85, and ChTnC were followed using mean residue ellipticity at 222 nm. The protein concentrations were 2.76 $\mu$M. The buffer solutions contained 10 mM MOPS, pH 7.25, 50 mM KCl, 1 mM DTT, and 1 mM EDTA. Panel A: apo-ChTnC1−85. Panel B: apo-ChTnC12−85. Panel C: ChTnC. Data points represent 15 s averages and were taken every 20 s. The data were fit to a two-state model of unfolding (eq 8). Parameters of the fits are in Table 2.

The $m_g$ parameters obtained from the LEM analysis presented in Table 4 are characteristic of the denaturant and the structure being unfolded via the surface area exposed upon unfolding and $\Delta C_p$ (Meyers *et al.*, 1995). The linear relationship between $\Delta C_p$ and $m_g$ (Alonzo & Dill, 1991) used to obtain $\Delta C_p$ for our fragments with similar structures confirms the linear correlation observed by Meyers *et al.* (1995). Using the correlations presented by Meyers *et al.* (1995), the values of $m_g$ we observed for urea and guanidine hydrochloride denaturation give $\Delta C_p$ values which are in qualitative agreement with the $\Delta C_p$ that we measured.

The legitimacy of the values of $\Delta G^o_{H_2O,25°C}$ that were derived from LEM analysis was assessed for apo ChTnC1−85 by a comparison with the results of CD thermal denaturations which is presented in Table 5. LEM analysis of the urea data generated a value of 2.7 kcal/mol for $\Delta G^o_{H_2O,25°C}$ while van't Hoff analysis of the thermal data gave a value of 2.6 kcal/mol; they are in excellent agreement. For all the fragments the values of $\Delta G^o_{H_2O,25°C}$ from LEM analysis using urea as a denaturant and from CD thermal denaturation agreed to within ≈0.5 kcal/mol.

In contrast to the general agreement between urea and thermal denaturation results for ChTnC1−85, analysis of denaturation experiments in GndHCl plus 0.5 M NaCl consistently generated values of $\Delta G^o_{H_2O,25°C}$ that were about 3 kcal/mol larger. Interestingly, this difference of 3 kcal/mol was observed for the other ChTnC N-domain fragments and RbTnC; in all cases, $\Delta G^o_{H_2O,25°C}$ for GndHCl denaturation in the presence of 0.5 M NaCl was ≈3 kcal/mol greater than $\Delta G^o_{H_2O,25°C}$ obtained from urea denaturations (see Table 4).

Our decision to include 0.5 M NaCl in protein samples for GndHCl titration was based on the results of a series of thermal denaturation experiments that were carried out in order to evaluate the effect of salt on the standard free energies of unfolding for the ChTnC N-domain fragments. ChTnC1−85 was chosen as a representative protein for these studies. The results, shown in Figure 7, indicate that apo-ChTnC1−85 is stabilized by concentrations of GndHCl up to ≈1 M with a peak effect at ≈0.3 M. To test the generality of this effect, thermal denaturations were carried out under two additional types of solution conditions: (1) increasing amounts of NaCl, and (2) increasing amounts of GndHCl in the presence of 0.5 M NaCl. NaCl has a significant stabilizing effect at low concentrations that plateaus at ≈0.5 M NaCl. The extrapolated standard free energy of thermal unfolding at 25 °C in the presence of 0.5 M NaCl ≈ 5.2 kcal/mol. In the presence of 0.5 M NaCl, GndHCl only destabilizes the protein. Similar results were obtained for the other ChTnC N-domain fragments; all reached plateau values of $\Delta G^o_{H_2O,25°C}$ at ≈0.5 M NaCl and 0.3 M GndHCl. The observed plateau for values of $\Delta G^o_{H_2O,25°C}$ in the presence of increasing [NaCl] suggests that the effect of NaCl on folding stability is saturable. This is likely due to the maximal possible screening of electrostatic interactions in the proteins. Based on the results that suggested that 0.5 M NaCl is the minimal amount of salt that is able to screen the stabilizing effects of GndHCl, we included 0.5 M NaCl in all GndHCl in unfolding experiments.

The effect of increasing salt on apo-ChTnC95−162 was to increase α-helical structure; most structure has formed when the concentration of NaCl is 1 M. The far-UV CD spectrum of apo-ChTnC95−162 in the presence of 2 M NaCl is similar to the spectrum in the presence of 0 M NaCl and 2 mM $CaCl_2$ (see Figure 1). This suggests that high concentrations of NaCl have induced α-helical structure comparable to that in the divalent ion-stabilized structure of ChTnC95−162.

*Effects of the N-Helix and the D/E Linker Region on Chemical Stability.* As was observed for the thermal denaturation experiments, the N-helix and the D/E linker regions stabilize ChTnC N-domain toward chemical denaturation. The trend in protein stabilities for the apo-N-domain fragments toward urea and GndHCl denaturation is same as for the thermal denaturation results. As with thermal denaturation results, the effect of N-helix deletion on $\Delta G^o_{H_2O,25°C}$ depends on the presence of the D/E linker region. It is of interest that the energetic effects of N-helix deletion from ChTnC1−85 ($\Delta\Delta G^o_{25}$ = −0.9 kcal/mol for urea denaturation, −0.8 kcal/mol for GndHCl denaturation) and D/E linker deletion from ChTnC1−105 ($\Delta\Delta G^o_{25}$ =

Table 3: Estimation of Calcium Association Constants for ChTnC N-Domain Fragments from Thermal Unfolding Data[a]

| protein[b] | [calcium] | $\Delta G^{o}_{25,Ca}$, kcal/mol[c] | $\Delta G^{o}_{25,Ca} - \Delta G^{o}_{25,Apo}$, kcal/mol[c] | calcd $K_{Ca}$,[d] $M^{-1}$ | exptl $K_{Ca}$,[e] $M^{-1}$ |
|---|---|---|---|---|---|
| ChTnC1−85 | 11.8 $\mu$M | 3.9 | 1.3 | $3.4 \times 10^5$ | $(2.4 \pm 0.1) \times 10^5$ |
| | 50 $\mu$M | 4.7 | 2.1 | $2.0 \times 10^5$ | |
| | 100 $\mu$M | 6.1 | 3.5 | $3.6 \times 10^5$ | |
| | 512 $\mu$M | 7.3 | 4.7 | $2.0 \times 10^5$ | |
| | 1 mM | 7.7 | 5.1 | $1.5 \times 10^5$ | |
| ChTnC12−85 | 50 $\mu$M | 3.7 | 2.1 | $2.0 \times 10^5$ | $(3.5 \pm 0.8) \times 10^5$ |
| | 70 $\mu$M | 4.1 | 2.5 | $2.2 \times 10^5$ | |
| | 100 $\mu$M | 4.4 | 2.8 | $2.0 \times 105$ | |
| ChTnC1−105 | 50 $\mu$M | 6.1 | 1.0 | $5.2 \times 10^4$ | $(8.6 \pm 1.4) \times 10^4$ |
| | 100 $\mu$M | 6.7 | 1.6 | $5.5 \times 10^4$ | |
| ChTnC12−105 | 100 $\mu$M | 5.5 | 5.5 | $1.6 \times 10^5$ | $1.9 \times 10^5$ |

[a] Ranges for parameters are ± student standard deviations. [b] Solution conditions: 10 mM MOPS, pH 7.25, 50 mM KCl, 1 mM DTT; the noted calcium concentrations refer to final concentrations of free calcium; protein concentrations were 2.76 $\mu$M. [c] Values of $\Delta G^{o}_{25,Apo}$ are taken from Table 2. Values of $\Delta G^{o}_{25,Ca}$ were calculated using the Gibbs−Helmholtz equation (eq 9). The values of $\Delta C_p$ used are given in Table 2. [d] Values of $K_{Ca}$ were calculated by equating $(\Delta G^{o}_{25,Ca} - \Delta G^{o}_{25,Apo})$ to the interaction free energy of calcium binding, $RT \ln(1/(1 + k_a[Ca^{2+}])^2)$, eq 14, where the logarithmic term is the binding polynomial that assumes identical and independent binding sites. In the table $K_{Ca} = 2k_a$. [e] Data from Table 1.

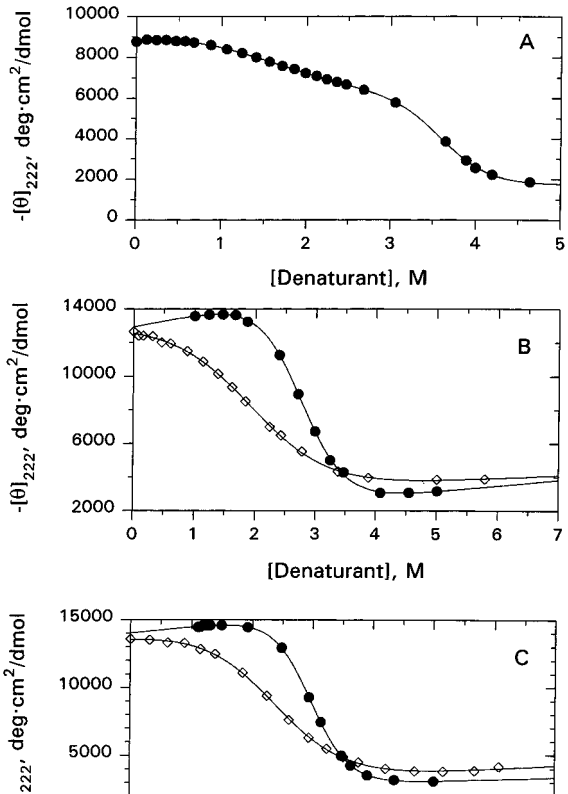


FIGURE 6: Chemical denaturation. Mean residue ellipticity at 222 nm was measured as a function of urea (◊) or GuHCl (●) at 25 °C. Protein solutions contained 10 mM MOPS, pH 7.25, 50 mM KCl, 1 mM DTT, and 1 mM EDTA. Solutions for all GndHCl titrations contained 0.5 M NaCl as well. The Linear Extrapolation Model was used to fit all curves (eq 6). Panel A: RbTnC. Panel B: ChTnC12−85. Panel C: ChTnC1−85.

−2.8 kcal/mol for urea denaturation, −2.9 kcal/mol for GndHCl denaturation) are essentially independent of the type of chemical denaturant.

*Effects of Domain Isolation.* Panel A of Figure 6 presents GndHCl denaturation data for apo-RbTnC. The unfolding profile for apo-RbTnC shows a broad transition, between ≈0.5 M GndHCl and 3 M GndHCl, followed by a steeper transition that extends to ≈4.5 M GndHCl. We have assigned the first broad transition to the unfolding of the C-domain of RbTnC based on low value for the $m_g$ parameter which is comparable to that for ligand-bound ChTnC95−162 (≈−1.0). A transition is observed for the C-domain because of the presence of a salt-induced structure. The steeper transition centered at ≈3.6 M GndHCl is assigned to the unfolding of the apo-N-domain. The $m_g$ slope parameter for this transition is in good agreement with those of ChTnC1−85 and ChTnC1−105.

The values of $\Delta G^{o}_{H_2O,25°C}$ for the apo-N-domain of RbTnC are 6.8 kcal/mol for GndHCl denaturation and 4.2 kcal/mol for urea denaturation. The difference in $\Delta G^{o}_{H_2O,25°C}$ for RbTnC and ChTnC1−105 is ≈1.7 kcal/mol for both urea and GndHCl data sets and reflects differences in the unfolding environment in the isolated domain. The difference in $\Delta G^{o}_{H_2O,25°C}$ for RbTnC and ChTnC1−85 is ≈1.2 kcal/mol for GndHCl denaturation and ≈1.5 kcal/mol for urea denaturation, also indicative of a different unfolding environment. Thus, in qualitative agreement with the thermal denaturation results, the stability of the N-domain of TnC toward chemical denaturation is affected by isolation as either ChTnC1−85 or ChTnC1−105. The apo-N-domain of ChTnC1−85 is stabilized on "incorporation" into holo-TnC by 1.2−1.5 kcal/mol while incorporation of the apo-ChTnC1−105 structure into holo-TnC destabilizes the N-domain. The magnitude of these effects is essentially independent of the type of chemical denaturant. Comparable data for the C-domain are not available due to the absence of structure in the ligand-free state.

## DISCUSSION

Five recombinant ChTnC fragments have been characterized using circular dichroism spectral measurements to monitor protein secondary structure, stability, and calcium binding. In addition to confirming the structural and functional integrity of these fragments, our results address important aspects of TnC structure and function, as well as more general aspects of the measurement of protein stability and its correlation with function.

Table 4: Chemical Stability Parameters for RbTnC and ChTnC Fragments

| solution conditions | parameters | ChTnC95−162 | ChTnC1−85 | ChTnC12−85 | ChTnC1−105 | ChTnC12−105 | RbTnC[f] |
|---|---|---|---|---|---|---|---|
| 2 mM EDTA | | | $n$[e] = 4 | $n = 3$ | $n = 3$ | $n = 2$ | $n = 2$ |
| | $\Delta G^{o}_{25,0.5M\ NaCl}$ [b] | NM | 5.6 ± 0.1 | 4.8 ± 0.4 | 8.5 ± 0.3 | 7.1 ± 0.1 | C: 2.2 ± 0.1<br>N: 6.8 ± 0.7 |
| | $-m_g$[c] | NM | 1.93 ± 0.03 | 1.75 ± 0.1 | 2.08 ± 0.05 | 1.95 ± 0.01 | C: 1.45 ± 0.25<br>N: 1.87 ± 0.23 |
| | $[GndHCl]_{1/2}$[d] | NM | 2.88 ± 0.06 | 2.76 ± 0.06 | 4.10 ± 0.06 | 3.63 ± 0.01 | C: 1.52 ± 0.04<br>N: 3.62 ± 0.06 |
| 2 mM EDTA | | | $n$[e] = 3 | $n = 3$ | $n = 1$ | $n = 2$ | $n = 2$ |
| | $\Delta G^{o}_{25,H_2O}$ [b] | NM | 2.7 ± 0.1 | 1.8 ± 0.1 | 5.5 | 3.8 ± 0.34 | N: 4.2 ± 0.5 |
| | $-m_g$[c] | NM | 1.16 ± 0.7 | 0.93 ± 0.04 | 1.01 | 0.93 ± 0.12 | N: 1.00 ± 0.09 |
| | $[urea]_{1/2}$[d] | NM | 2.35 ± 0.07 | 1.92 ± 0.04 | 5.44 | 4.14 ± 0.17 | N: 4.15 ± 0.12 |

[a] Ranges for parameters are ± student standard deviation. NM: not measured. [b] Units of $\Delta G^{o}_{25,x}$ = kcal/mol. [c] Units of $m_g$ = kcal/(mol·M GndHCl). [d] Calculated as $\Delta G^{o}_{25,x}/m_g$. [e] Number of trials. [f] The designations N and C refer to the N-terminal and C-terminal domains, respectively, of RbTnC.

Table 5: Comparison of Chemical and Thermal Denaturation Data for Apo-ChTnC1−85[a]

| GndHCl | GndHCl @ 0.5 M NaCl | urea | CD thermal |
|---|---|---|---|
| $\Delta G^{o}_{25,H_2O}$ [b,c] = 5.2 | $\Delta G^{o}_{25,H_2O} = 5.6 \pm 0.1$ | $\Delta G^{o}_{25,H_2O} = 2.7 \pm 0.1$ | $\Delta G^{o}_{25,H_2O}$ [b] $= 2.6 \pm 0.1$ |
| $m_g$[c] = −2.1 | $m_g = -1.93 \pm 0.03$ | $m_g = -1.16 \pm 0.07$ | $\Delta H^{o}_{vh,25} = 37.5 \pm 1.1$ |
| $[GdnHCl]_{1/2}$[c] = 2.47 M | $[GdnHCl]_{1/2} = 2.88 \pm 0.06$ M | $[urea]_{1/2} = 2.35 \pm 0.07$ M | $T_m = 318.4 \pm 0.4$ K |
| $n$[d] = 1 | $n = 4$ | $n = 3$ | $n = 7$ |

[a] Solution conditions for CD thermal and chemical denaturation experiments: 10 mM MOPS, pH 7.25, 50 mM KCl, 2 mM EDTA; 0.5 M NaCl was included as noted. Protein concentrations were 2.76 $\mu$M for CD thermal denaturation experiments and 15 $\mu$M for chemical denaturation experiments. Ranges for parameters are ± student standard deviations. [b] Units of $\Delta G^{o}_{25,x}$ = kcal/mol; values for thermal stability were calculated using eq 9 and appropriate values of $\Delta C_p$ listed in Table 2. Values for chemical stability are fit parameters from LEM analysis of chemical denaturation data (eq 6). [c] Parameters from LEM analysis of chemical denaturation are taken from Table 4; units of $m_g$ = kcal/(mol·M GndHCl). [d] Number of trials. [e] Units of $\Delta H^{o}_{vh,25}$ = kcal/mol; values calculated using eq 10.

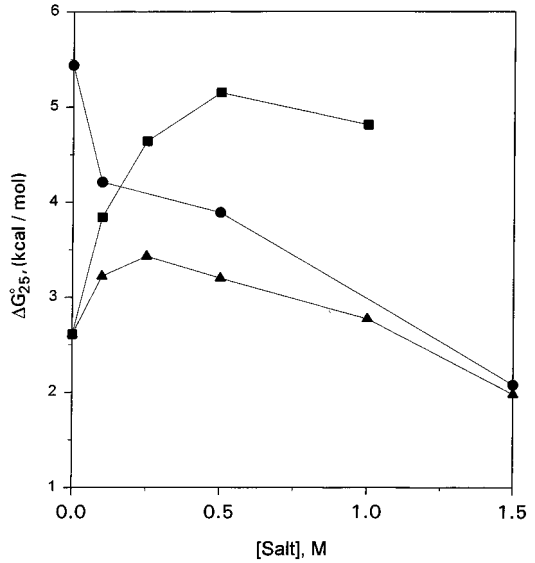


FIGURE 7: Effects of NaCl and GndHCl on the thermal stability of apo-ChTnC1−85. Each data point represents a single thermal unfolding experiment performed at the indicated salt concentration. Other components are listed in the legend to Figure 5. NaCl (■); GndHCl (▲); GndHCl + 0.5 M NaCl (●). The values of $\Delta G^{o}_{25}$ were calculated using eq 9 and a $\Delta C_p$ of 260 cal/(mol·K) which was measured from data of preliminary DSC experiments carried out in the presence of 0.5 M NaCl.

The CD spectra of the apo-N-domain mutants (examples shown in Figure 1) indicate that all have significant α-helical content, which is lost on thermal or chemical unfolding, consistent with earlier results on related fragments (Leavis *et al.*, 1978; Li *et al.*, 1994). The molar ellipticities of our fragments compare well with those of similar fragments described in the literature. Small differences persist which reflect the structural effects of deletions (N-helix or D/E linker region) and/or the positioning and differing numbers of aromatic residues (Woody, 1994; Manning & Woody, 1989). Neither fragmentation of the molecule nor our tyrosine substitutions significantly affected the folded structure of the N-domain of ChTnC as indicated by the near identity of the van't Hoff enthalpies for apo-ChTnC1−85 and ChTnC unfolding (Table 2) and recent structural work (Li *et al.*, 1994; Gagné *et al.*, 1994, 1995).

Magnesium binding to the N-domain of TnC is suggested by the altered CD spectra of apo-TnC1−85 and apo-ChTnC1−105 in 20 mM $MgCl_2$. This is consistent with NMR results of Tsuda *et al.* (1990) and is substantiated by our stability studies from which we determined a $K_{Mg}$ of ≈440 $M^{-1}$ for ChTnC1−85 (calculated using eq 14).

The folding of apo-ChTnC95−162, indicated by large ligand-dependent changes in $[\theta]_{222nm}$ (Figure 1), confirms its identity as the calcium/magnesium binding domain of ChTnC. The changes in ellipticity we observed for magnesium and calcium binding to ChTnC95−162, ≈−8970 and −9810 deg·cm²·dmol$^{-1}$, respectively, are in agreement with those reported by Leavis *et al.* (1978) for calcium binding to the nearly identical TR2 fragment of RbTnC. These changes are in agreement the early calorimetric work of Tsalkova and Privalov (1985) and recent spectroscopic work of Li *et al.* (1994) and Smith *et al.* (1994) which suggest structural differences between the calcium- and magnesium-bound forms of the protein.

### *Protein Stability*

*Reversibility and Two-State Unfolding.* Our results suggest that thermal and chemical unfolding of the recombinant

ChTnC fragments, as well as apo-RbTnC, are reversible as indicated by signal recovery and two state as is suggested by the observed isodichroic points near 204 nm for the temperature-dependent CD spectra. Preliminary DSC results for apo-ChTnC1−85 give a ratio for $\Delta H_{vh}$:$\Delta H_{cal}$ that is close to one, consistent with the earlier DSC results of Tsalkova and Privalov (1985) which also indicated a two-state thermal transition for this domain of apo-TnC. An indicator of two-state unfolding for urea and thermal denaturation is the good agreement between extrapolated values of $\Delta G^o_{25}$ for these two methods. In our studies we have assumed that GndHCl-induced unfolding also follows a two-state mechanism as all our data are well fit by this model. Residual plots for fits of all data (thermal and chemical denaturations) to a two-state model show no significant nonrandom trends; this indicates that two-state analysis (using the LEM or van't Hoff analysis) adequately describes the data.

*Thermal Stability: C-Terminal Fragment, ChTnC95−162.* Like the C-domain (calcium−magnesium domain) of apo-TnC, apo-ChTnC95−162 appears to be devoid of significant helical or tertiary structure. We did not observe an unfolding transition for this fragment in agreement with previous calorimetric work (Tsalkova & Privalov, 1980, 1985). Folding and calcium binding are tightly linked processes for this protein fragment. The $3^1/_2$-fold increase in $[\theta]_{222nm}$ (see Figure 1) along with the appearance of a distinct thermal transition in the CD (see Table 2 and Figures 1 and 3) bear this out. The extrapolated van't Hoff enthalpy at 25 °C for $Ca_2$-ChTnC95−162 is ≈20 kcal/mol less than that for the apo-ChTnC1−*x* fragments and the N-domain of apo-ChTnC; this suggests a looser, more open structure for this ligand-bound C-domain fragment as compared to the apo-N-domain fragments.

The $\Delta G^o_{25}$ value of ≈−1.8 kcal/mol (approximately 95% unfolded) that we calculated from the free energy of unfolding measured in the presence of various concentrations of calcium ion and the calcium binding constants for apo-ChTnC95−162 by eq 14 is entirely consistent with results of our CD spectral and thermal denaturation data. To our knowledge, this is the first quantitative estimate of the folding stability of the ligand-free form of the troponin C C-domain.

*Thermal Stability: Apo-N-Domain ChTnC Fragments. (A) Effect of Domain Isolation.* In comparing values of $\Delta G^o_{25}$ in Table 2, it is apparent that the stability of the apo-N-domain (i.e., ChTnC1-85) is significantly affected by the presence of sequentially more distant parts of apo-TnC in addition to the N-helix. For example, the $\Delta G^o_{25}$ for the N-domain is larger in ChTnC1−105 and RbTnC, 5.1 and 4.8 kcal/mol, respectively, vs 2.6 kcal/mol for ChTnC1−85. This observation is suggestive of interactions between TnC domains and is consistent with results of several other groups that have shown that calcium binding to the C-terminal domain of holo-TnC affects spectroscopic probes in the N-domain (Wang *et al.*, 1990; Grabarek *et al.*, 1986, 1992; Tsuda *et al.*, 1988; Li et al., 1994). Results of DSC experiments on tryptic fragments of rabbit TnC have been interpreted to suggest the presence of a destabilizing interaction between the two functional domains of holo-TnC (Tsalkova & Privalov, 1985).

While differing in folding stability, the near-equal values of $\Delta H^o_{vh,25}$ for ChTnC, RbTnC, ChTnC1−105, and ChTnC1−85 in Table 2 suggest that the global structure of the apo-N-domain within the fragments is similar. It is impossible to know, based on these data, if the stabilizing forces within apo-TnC are similar to those within apo-ChTnC1−105. It is noteworthy, however, that the free energy of unfolding for the apo-N-terminal domain of holo-ChTnC and ChTnC1−105 are similar and are each approximately 2.3 kcal/mol greater than that for apo-ChTnC1−85.

(*B) Effects of D/E Linker Region and N-Helix.* Addition of residues 86−105 to the apo-ChTnC1−85 fragment results in a $\Delta\Delta G^o_{25}$ of ≈2.5 kcal/mol. The stabilizing effects of residues 86−105 for the ChTnC12−85 fragment are smaller with $\Delta\Delta G^o_{25}$ ≈ 1.3 kcal/mol. This suggests that the D/E linker region interacts with the globular portion of the ChTnC*x*−105 fragments.

Deletion of the N-helix from the ChTnC1−*x* fragments results in decreased values of $\Delta G^o_{25}$ and $\Delta H^o_{vh,25}$. This result is not unexpected in view of the crystal structure of this domain within holo-TnC. The N-helix is part of a four-helix barrel that encloses the D-helix. Seven of eleven residues of the D-helix (residues 74−85) within the protein core are hydrophobic. Deletion of the N-helix deletion would likely expose a significant portion of the hydrophobic protein interior to solvent and, thus, destabilize the protein. The apparent stability penalty due to N-helix deletion from the apo-N-domain of ChTnC1−85 is increased by ≈1.2 kcal/mol when the D/E linker region is present. This implies that at least part of the stabilizing effect of the D/E linker region involves an interaction, be it direct or indirect, with the N-helix. These results are consistent with those of Smith *et al.* (1994) in their study of N-helix-deletion mutants of holo-ChTnC.

Several reports have presented stability data, in terms of thermal transition midpoints ($T_m$), for TnC and TnC mutants (McCubbin *et al.*, 1980; Tsalkova & Privalov, 1980, 1985; Dobrowolski *et al.*, 1991a,b; Smith *et al.*, 1994; Grabarek *et al.*, 1995; Ramakrishnan & Hitchcock-DeGregori, 1995). In recent stability studies of an N-helix-deletion mutant of ChTnC, CnTnCΔ14, Smith *et al.* (1994) reported a decrease in $T_m$ of ≈20 °C in the presence and absence of a magnesium-bound C-domain. This 20 °C decrease in $T_m$ is to be compared with the ≈10 °C decrease in $T_m$ we observed for deletion of the N-helix from ChTnC1−105; a decrease in $T_m$ of ≈3.5 °C was observed due to N-helix deletion from ChTnC1−85 (see Table 3). This suggests an even larger role for the N-helix in N-domain stability within the context of the holoprotein. Taken together, these results point to a significant interaction between the N-helix and residues of holo-TnC (apo or magnesium bound) which are C-terminal to residue 85 that are important for apo-N-domain stability.

In summary, our thermal denaturation results suggest that the structure of the N-domain of TnC is not significantly affected by isolation as a protein fragment; it is, however, stabilized by residues that are C-terminal to residue 85. Deletion of the N-helix decreases protein stability in a way that depends on the presence of residues that are C-terminal to residue 85. Our results yielded a value of $\Delta G^o_{25} = -1.8$ kcal/mole for apo-ChTnC95−162; this first quantitative estimate is consistent with spectral and calorimetric data which indicate that the ligand-free C-domain of TnC is mostly unfolded at 25 °C.

*Chemical Denaturation Studies. (A) Comparison with Thermal Denaturation.* The observed trends in the overall

stability for chemical denaturation parallel those for thermal denaturation for the troponin C fragments. Deletion of the N-helix from ChTnC1−85 destabilizes the N-domain by 0.8 kcal/mol, addition of residues 86−105 stabilizes the N-domain by ≈3 kcal/mol, and the effect of each depends on the presence of the other; this indicates the presence of an interaction between the N-helix and the D/E linker sequence in ChTnC1−105. These effects are noted for both urea and GndHCl denaturation.

In addition, isolation of the N domain as ChTnC1−85 significantly decreased $\Delta G^{o}_{25}$ by ≈1.50 kcal/mol for both urea and GndHCl denaturation, indicative of the removal of stabilizing interactions between the N-domain and region(s) of ChTnC sequence spanning residues 86−162. Deletion of the N-helix from either ChTnC1−85 or ChTnC1−105 decreased the cooperativity of unfolding transitions based on changes in the $m_g$ parameter of the Linear Extrapolation Model; this parallels the trend noted for $\Delta H^{o}_{vh,25}$ (Table 2) from thermal denaturation experiments (Meyers *et al.*, 1995).

Our data also show that values of $\Delta G^{o}_{25}$ derived from urea and heat denaturation experiments are in quantitative agreement (Table 5). In comparing urea with thermal unfolding data from Tables 4 and Table 2, the values of $\Delta G^{o}_{25}$ for ChTnC12−85 and ChTnC1−105 agree quite well. This suggests that, for TnC fragments, chemical denaturation using urea is able to accurately measure the free energy of unfolding, $\Delta G^{o}_{25}$. The apparent difference in values of $\Delta G^{o}_{25}$ for ChTnC12−105 is likely due to larger error in LEM analysis of curves with abbreviated denatured baselines.

*(B) Electrostatic Free Energy.* That the free energies of unfolding determined from urea and GndHCl experiments are very different speaks to the significant role of electrostatic interactions in the stability of TnC. We have calculated the net electrostatic contribution to $\Delta G^{o}_{25}$ for the globular domains of TnC following Monera *et al.* (1994) who have demonstrated the utility of urea and GndHCl denaturation data for this purpose. The important underlying assumption is that urea denaturation is sensitive to all types of physicochemical interactions that contribute to protein stability (affirmed by the excellent agreement between $\Delta G^{o}_{25}$ values derived from urea and thermal unfolding experiments) while GndHCl, in the presence of 0.5 M NaCl, is sensitive to nonelectrostatic interactions. In our opinion, the near-constant value of ≈−3.0 kcal/mol for the difference between $\Delta G^{o}_{25,urea}$ and $\Delta G^{o}_{25,GuHCl}$ for the N domain fragments accurately reflects the net electrostatic contribution to the N-domain. Since this value is not affected by the presence or absence of the N-helix and D/E linker structures, the main source of the destabilizing electrostatic interactions in these proteins is inherent in their common globular structure, i.e., the carboxyl ligands of the EF hand calcium binding motif. The value of −3.00 kcal/mol is also a reasonable estimate for the net electrostatic contribution to stability of the C-domain of TnC.

That destabilizing electrostatic interactions reduce the structural stability of the C-domain of TnC is demonstrated by the ability of NaCl to induce secondary and tertiary structure in ChTnC95−162 by electrostatic screening effects. In obvious contrast to the stable N-domain of TnC, stabilizing nonelectrostatic (hydrophobic) interactions do not compensate for destabilizing electrostatic interactions in the apo-TnC C-domain. A qualitative explanation for this lack of stabilizing hydrophobic interactions is the absence, in the C-domain, of a predominately hydrophobic stretch of α-helical structure that could serve as a nucleus for a hydrophobic core. In the N-domain, the D-helix contains many hydrophobic amino acid residues which are surrounded by the N-helix and the A, B, and C helices in a four-helix "bundle" structure. The increased stability of the TnC C-domain observed at lower pH supports these conclusions (Ingraham & Swenson, 1983). A recent report showed that increase in negative charge by acetylation of RbTnC decreased stability in agreement with our results (Grabarek *et al.*, 1995). A design consideration for these calcium binding domains is that negative charges in close proximity must be allowed and, further, the positive charge on the protein should be distributed so as to achieve the desired calcium binding constants via adjustments of the calcium off-rate (Falke *et al.*, 1994; Drake & Falke, 1996).

In addition to facilitating an estimation of the net electrostatic contribution to protein stability, differences in $\Delta G^{o}_{25}$ values derived from urea and GndHCl unfolding experiments permit a qualitative assessment of the stabilizing effects of the N-helix and the D/E linker sequence (and perhaps the C-domain) on the stability of the N-domain. The destabilizing effect of N-helix deletion from ChTnC1−85 is ≈−1.0 kcal/mol for urea-, thermal-, and GndHCl-induced unfolding. For ChTnC1−105 the energetic penalty of N-helix deletion depends, somewhat, on the unfolding perturbant; for urea denaturation, thermal denaturation, and GndHCl denaturation the decreases in stability are ≈1.69, ≈2.19, and ≈1.41 kcal/mol, respectively. We interpret this to mean that the contribution of the N-helix to N-domain stability is mainly hydrophobic in nature. The significant stabilizing effect of the D/E linker sequence in ChTnC1−105 seems to have a predominately hydrophobic character with a small electrostatic component.

*TnC Structure and Energetics.* Isolation of the N-domain is expected to affect folding stability. These results are consistent with the previously observed positive interaction free energy for the binding of TnC to TnI in the presence and absence of divalent metal ions (Swenson & Fredricksen, 1992). In this earlier work we concluded that domain separation increased the binding affinity for TnI and decreased the calcium dependence of the interaction. The interdomain interaction that affects TnC affinity for TnI would necessarily be manifested in altered folding stabilities of isolated TnC domains. By virtue of the direct effects on the folding stability of the ligand-free N-domain, the N-helix and the bilobed domain organization of TnC are necessarily involved in the fine-tuning of the affinity and cooperativity of calcium binding and, hence, the fine tuning of all of the calcium-dependent interactions within the regulated thin filament. Though not directly involved in the chemical coordination of calcium ions, these structural features are critically important for the function of TnC as a switch for regulating muscle contraction. In support of this idea, the results of NMR studies of Shaw *et al.* (1991) convincingly demonstrated how noncoordinating residues in TnC calcium-binding loops can dramatically affect calcium affinity.

Changes in the folding stability are expected to affect ligand binding of an apoprotein. Increased stability of a ligand-free protein conformation ought to decrease ligand affinity due to increased resistance to the required structural

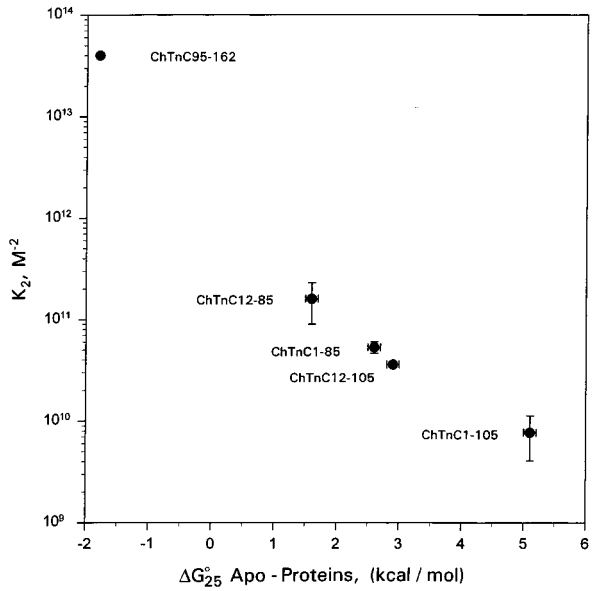


FIGURE 8: Free energy of unfolding, $\Delta G^{\circ}_{25}$, and calcium affinity $K_2$. Values of $K_2$ are plotted on a logarithmic ordinate versus $\Delta G^{\circ}_{25}$, the free energy of thermal unfolding for apoproteins, which is taken from Table 2. The value of $\Delta G^{\circ}_{25}$ for apo-ChTnC95−162 was estimated as discussed in the text. The error bars represent student standard deviations. The error bars for ChTnC95−162 are within the data point.

change to accommodate the ligand. We note in our work that folding stability tracks with calcium-binding parameters which include binding cooperativity ($K_a$, $H_a$: Model A; and $K_2$, $\Delta G_c$: Model B) (see Figure 8). The cooperative effects noted in $K_a$ of Model A are mirrored by those of $K_2$ of Model B. Cooperativity effects are not noted for $K_1$ as it measures primarily binding of the first ligand. It is interesting to note that Grabarek *et al.* (1995) noted that decreased stability of the TnC N-domain was accompanied by increased calcium affinity. Our observations suggest a very basic relationship between the stability of a protein with 2 ligand-binding sites and the cooperativity of ligand binding and, hence, the ability of the protein to respond to changes in ligand concentration. The requirement for a particular calcium affinity and level of binding cooperativity in the molecular switch, TnC, is partly fulfilled by the energetic effects of the N-helix and the bilobed domain organization of the protein.

In summary, we have characterized the calcium-binding and folding stability of five novel recombinant fragments of ChTnC. The results of urea and thermal denaturation of the N-domain are in good quantitative agreement. The differences in $\Delta G^{\circ}_{25}$ derived from urea or thermal and GndHCl denaturations represent good, quantitative estimates of the contribution of electrostatic interactions to protein stability; this amounts to $\approx -3.0$ kcal/mol of destabilization for all of these proteins. Our data provide the first estimate of the $\Delta G^{\circ}_{25}$ of the apo-C-domain of TnC of −1.8 kcal/mol; this result is consistent with the qualitative spectral and calorimetric data reported that show little structure for this domain at 25 °C. The inverse relationship noted between cooperative binding free energy and folding stability of an apoprotein speaks to the critical role that protein stability plays in protein function. Thus, our results suggest subtle yet significant roles for the N-helix and the bilobed structure of TnC in determining ligand affinity, structural stability, and, hence, appropriate function of troponin C as part of a molecular switch.

## ACKNOWLEDGMENT

We thank Dr. Sara Hitchcock-DeGregori for providing us with the cDNA used for cloning the troponin C fragments. We thank Dr. Daniel Weeks for assistance in performing all aspects of the cloning. We acknowledge the Protein Structure Facility of the College of Medicine of the University of Iowa for the use of the Aviv Model 62 DS circular dichroism spectrometer, the Aviv 14DS UV−vis−IR spectrometer, and the SLM4800C fluorometer. We acknowledge the laboratory of Dr. Kenneth Murphy for the use of the modified DASM 1 calorimeter. We acknowledge Dr. David Price for the use of Tablecurve in data analysis.

## REFERENCES

Alonso, D. O. V., & Dill, K. A. (1991) *Biochemistry 30*, 5974−5985.
Babu, A., Rao, V. G., Su, H., & Gulati, J. (1993) *J. Biol. Chem. 268*, 19232−19238.
Blechner, S. L., Olah, G. A., Strynadka, N. C. A., Hodges, R. S., & Trewhella, J. (1992) *Biochemistry 31*, 11326−11334.
Bolen, D. W., & Santoro, M. M. (1988) *Biochemistry 27*, 8069−8074.
Cachia, P. J., Sykes, B. D., & Hodges, R. S. (1983) *Biochemistry 22*, 4145−4152.
Chandra, M., da Silva, A. C. R., Sorenson, M. M., Ferro, J. A., Pearlstone, J. R., Nash, B. E., Borgford, T., Kay, C. M., & Smillie, L. B. (1994) *J. Biol. Chem. 269*, 14988−14994.
Cheung, H. C., Wang, C., & Malik, N. A. (1987) *Biochemistry 26*, 5904−5907.
Dalgarno, D. C., Grand, R. J. A., Levine, B. A., Moir, A. J., Scott, G. M., & Perry, S. V. (1982) *FEBS Lett. 150*, 54−58.
da Silva, E. F., Sorenson, M. M., Smillie, L. B., Barrabin, H., & Scofano, H. M. (1993) *J. Biol. Chem. 268*, 26220−26225.
Dobrowolski, Z., Xu, G., Chen, W., & Hitchcock-DeGregori, S. E. (1991a) *Biochemistry 30*, 7089−7096.
Dobrowolski, Z., Xu, G., & Hitchcock-DeGregori, S. E. (1991b) *J. Biol. Chem. 266*, 5703−5710.
Drake, S. K., & Falke, J. J. (1996) *Biochemistry 35*, 1753−1760.
Falke, J. J., Drake, S. K., Haz, A. L., & Peerson, O. B. (1994) *Q. Rev. Biophys. 27*, 219−220.
Farah, C. S., Miyamoto, C. A., Ramos, C. H .I., da Silva, A. C., Quaggio, R. B., Fujimori, K., Smillie, L. B., & Reinach, F. C. (1994) *J. Biol. Chem. 269*, 5230−5240.
Gagne, S. M., Tsuda, S., Li, M., Chandra, M., Smillie, L. B., & Sykes, B. D. (1994) *Protein Sci. 3*, 1961−1974.
Gagne, S. M., Tsuda, S., Li, M., Smillie, L. B., & Sykes, B. D. (1995) *Nature, Struct. Biol. 2*, 784−789.
Gill, S. C., & von Hippel, P. H. (1989) *Anal. Biochem. 182*, 319−326.
Golosinska, K., Pearlstone, J. R., Borgford, T., Oikawa, K., Kay, C. M., Carpenter, M. R., & Smillie, L. B. (1991) *J. Biol.Chem. 266*, 15797−15809.
Grabarek, Z., Drabikowski, W., Leavis, P. C., Rosenfeld, S., & Gergely, J. (1981) *J. Biol. Chem. 256*, 13121−13127.
Grabarek, Z., Leavis, P. C., & Gergely, J. (1986) *J. Biol. Chem. 261*, 608−613.
Grabarek, Z., Tao, T., & Gergely, J. (1992) *J. Muscle Res. Cell Motil. 13*, 383−393.
Grabarek, Z., Mabuchi, Y., & Gergely, J. (1995) *Biochemistry 34*, 11872−11881.
Gulati, J., Babu, A., & Su, H. (1992) *J. Biol. Chem. 267*, 25073−25077.
Gulati, J., Babu, A., Su, H., & Zhang, Y. F. (1993) *J. Biol. Chem. 268*, 11685−11690.
Gulati, J., Akella, A. B., Su, H., Mehler, E. L., & Weinstein, H. (1995) *Biochemistry 34*, 7348−7355.
Herzberg, O., & James, M. N. G. (1985) *Nature 313*, 653−659.
Herzberg, O., & James, M. N. G. (1988) *J. Mol. Biol. 203*, 761−779.
Ingraham, R. H., & Swenson, C. A. (1983) *Eur. J. Biochem. 132*, 85−88.

Ingraham, R. H., & Swenson, C. A. (1984) *J. Biol. Chem. 259*, 9544−9548.
Johnson, J. D., Collins, J. H., & Potter, J. D. (1978) *J. Biol. Chem. 253*, 6451−6458.
Kretsinger, R. H., & Nockolds, C. E. (1973) *J. Biol. Chem. 248*, 3313−3326.
Laemmli, V. K. (1970) *Nature 227*, 680−685.
Leavis, P. C., & Gergely, J. (1984) *CRC Crit. Rev. Biochem. 16*, 235−289.
Leavis, P. C., Rosenfeld, S. S., Gergely, J., Grabarek, Z., & Drabikowski, W. (1978) *J. Biol. Chem. 253*, 5452−5459.
Li, M. X., Chandra, M., Pearlstone, J. R., Racher, K. I., Trigo-Gonzalez, G., Borgford, T., Kay, C. M., & Smillie, L. B. (1994) *Biochemistry 33*, 917−925.
Li, M. X., Gagne, S. M., Tsuda, S., Kay, C. M., Smillie, L. W., & Sykes, B. D. (1995) *Biochemistry 34*, 8330−8340.
Maniatis, T., Fritsch, E. F., & Sambrook, J. (1989) in *Molecular Cloning—A Laboratory Manual*, Cold Spring Harbor Laboratory Press, Cold Spring Harbor, NY.
Manning, M. C., & Woody, R. W. (1989) *Biochemistry 28*, 8609−8613.
Margossian, S. S., & Stafford, W. F., III (1982) *J. Biol. Chem. 257*, 1160−1165.
McCubbin, W. D., Hincke, M. T., & Kay, C. M. (1980) *Can. J. Biochem. 58*, 683−691.
Monera, O. D., Kay, C. M., & Hodges, R. S. (1994) *Protein Sci. 3*, 1984−1991.
Morjana, N. A., McKeone, B. J., & Gilbert, H. F. (1993) *Proc. Natl. Acad. Sci. U.S.A. 90*, 2107−2111.
Myers, J. K., Pace, C. N., & Scholtz, J. M. (1995) *Protein Sci. 4*, 2138−2148.
Negele, J. C., Dotson, D. G., Liu, W., Sweeney, H. L., & Putkey, J. A. (1992) *J. Biol. Chem. 267*, 825−831.
Olah, G. A., & Trewhella, J. (1994) *Biochemistry 33*, 12800−12806.
Pearlstone, J. R., Borgford, T., Chandra, M., Oikawa, K., Kay, C. M., Herzberg, O., Moult, J., Herklotz, A., Reinach, F. C., & Smillie, L. W. (1992) *Biochemistry 31*, 6545−6553.
Perrin, D. D., & Sayce, J. G. (1967) *Talanta 14*, 833−842.
Potter, J. D. (1982) *Methods Enzymol. 85*, 241−263.
Potter, J. D., & Gergely, J. (1975) *J. Biol. Chem. 250*, 4628−4633.
Potter, J. D., & Johnson, J. D. (1982) in *Calcium & Cell Function* (Cheung, W., Ed.) Vol. 2, pp 145−172, Academic Press, New York.
Ramakrishnan, S., & Hitchcock-DeGregori, S. E. (1995) *Biochemistry 34*, 16789−16796.
Sambrook, J., Fritsch, E. F., & Maniatis, T. (1989) in *Molecular Cloning—A Laboratory Manual*, 2nd ed., Cold Spring Harbor Laboratory Press, Cold Spring Harbor, NY.
Santoro, M. M., & Bolen, D. W. (1992) *Biochemistry 31*, 4901−4907.
Santoro, M. M., & Bolen, D. W. (1995) *Biochemistry 34*, 3771−3781.
Schellman, J. A. (1975) *Biopolymers 14*, 999−1018.
Schwarz, F. P. (1989) *Thermochim. Acta 147*, 71−91.
Shaw, G. S., Hodges, R. S., & Sykes, B. D. (1991) *Biochemistry 30*, 8339−8347.
Sheng, Z., Francois, J., Hitchcock-DeGregori, S. E., &, Potter, J. D. (1991) *J. Biol. Chem. 266*, 5711−5715.
Sillen, L. G., & Martell, A. E. (1964) *Spec. Publ.—Chem. Soc. 17*, 754.
Slupsky, C. M., & Sykes, B. D. (1995) *Biochemistry 34*, 15953−15694.
Smith, L. (1995) *Biophys. J. 68*, A57.
Smith, L., Greenfield, N. J., & Hitchcock-DeGregori, S. E. (1994) *J. Biol. Chem. 269*, 9857−9863.
Strynadka, N., & James, M. (1990) *Proteins: Struct., Funct., Genet. 7*, 234−248.
Studier, F. W., Rosenberg, A. H., Dunn, J. J., & Dubendorff, J. W. (1990) *Methods Enzymol. 185*, 60−89.
Swenson, C. A., & Fredricksen, R. S. (1992) *Biochemistry 31*, 3420−3429.
Talbot, J. A., & Hodges, R. S. (1981) *J. Biol. Chem. 256*, 2798−2802.
Trigo-Gonzalez, G., Racher, K., Burtnick, L., & Borgford, T. (1992) *Biochemistry 31*, 7009−7015.
Trigo-Gonzalez, G., Awang, G., Racher, K., Neden, K., & Borgford, T. (1993) *Biochemistry 32*, 9826−9831.
Tsalkova, T. N., & Privalov, P. L. (1980) *Biochim. Biophys. Acta 624*, 196−204.
Tsalkova, T. N., & Privalov, P. L. (1985) *J. Mol. Biol. 181*, 533−544.
Tsuda, S., Hasagawa, Y., Yagi, K., & Hikichi, K. (1988) *Biochemistry 27*, 4120−4126.
Tsuda, S., Ogura, K., Hasegawa, Y., Yagi, K., & Hikichi, K. (1990) *Biochemistry 29*, 4951−4958.
Van Eyk, J. E., & Hodges, R. S. (1988) *J. Biol. Chem. 263*, 1726−1732.
Waltersson, Y., Linse, S., Brodin, P., & Grundstrom, T. (1993) *Biochemistry 32*, 7866−7871.
Wang, C., & Chueng, H. C. (1985) *Biophys. J. 48*, 727−739.
Wang, Z., Sarkar, S., Gergely, J., & Tao, T. (1990) *J. Biol. Chem. 265*, 4953−4957.
Woody, R. (1994) *Eur. Biophys. J. 23*, 253−262.
Xu, G., & Hitchcock-DeGregori, S. E. (1988) *J. Biol. Chem. 263*, 13962−13969.
Yao, M., & Bolen, D. W. (1995) *Biochemistry 34*, 3771−3781.
Zot, H. G., & Potter, J. D. (1982) *J. Biol. Chem. 257*, 7678−7683.
Zot, H. G., & Potter, J. D. (1987) *Annu. Rev. Biophys. Biophys. Chem. 16*, 535−559.

BI961270Q